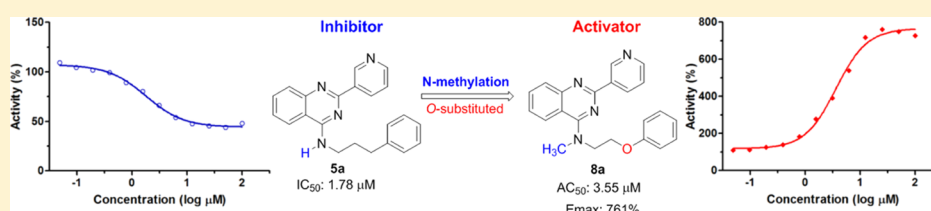


Conversion of Quinazoline Modulators from Inhibitors to Activators of β -GlucocerebrosidaseJianbin Zheng,^{†,‡} Sohee Jeon,[‡] Weilan Jiang,[‡] Lena F. Burbulla,[‡] Daniel Ysselstein,[‡] Kristine Oevel,[‡] Dimitri Krainc,^{*,‡,†} and Richard B. Silverman^{*,†,†}[†]Department of Chemistry, Chemistry of Life Processes Institute, Center for Molecular Innovation and Drug Discovery, and Center for Developmental Therapeutics, Northwestern University, Evanston, Illinois 60208, United States[‡]Department of Neurology, Northwestern University Feinberg School of Medicine, Chicago, Illinois 60611, United States

S Supporting Information



ABSTRACT: Gaucher's disease is a lysosomal disease caused by mutations in the β -glucocerebrosidase gene (*GBA1* and GCCase) that have been also linked to increased risk of Parkinson's disease (PD) and Diffuse Lewy body dementia. Prior studies have suggested that mutant GCCase protein undergoes misfolding and degradation, and therefore, stabilization of the mutant protein represents an important therapeutic strategy in synucleinopathies. In this work, we present a structure–activity relationship (SAR) study of quinazoline compounds that serve as inhibitors of GCCase. Unexpectedly, we found that N-methylation of these inhibitors transformed them into GCCase activators. A systematic SAR study further revealed that replacement of the key oxygen atom in the linker of the quinazoline derivative also contributed to the activity switch. PD patient-derived fibroblasts and dopaminergic midbrain neurons were treated with a selected compound (**9q**) that partially stabilized GCCase and improved its activity. These results highlight a novel strategy for therapeutic development of noninhibitory GCCase modulators in PD and related synucleinopathies.

INTRODUCTION

Gaucher's disease (GD), an autosomal recessive lysosomal storage disorder, is caused by mutations of the *GBA1* gene encoding the lysosomal enzyme β -glucocerebrosidase (GCCase). Mutations in *GBA1* were also found as a major risk factor for Parkinson's disease (PD) and dementia with Lewy bodies (DLB).^{1–5} Most of these mutations, including the prevalent N370S mutation, are still functional, although with low residual GCCase activity.⁶ Loss of function of GCCase leads to accumulation of glucosylceramide (GluCer),^{7,8} which also promotes the formation and stabilization of α -synuclein oligomers.⁹ Enhancement of GCCase activity is thought to be a potential therapeutic strategy for GCCase-associated synucleinopathies, including PD.^{10,11}

Several different scaffolds of non-iminosugar GCCase inhibitors have been reported as GCCase pharmacological chaperones (PCs) since 2007^{12–16} (Figure 1). We found that a noninhibitory GCCase PC NCGC00188758 (**2**)¹⁷ can enhance GCCase activity specifically within the lysosomal compartment, reduce GluCer and hexosylsphingosine substrates, and subsequently enhance the clearance of pathological α -synuclein.¹⁸ These findings suggested that reduction of GluCer may provide benefit in PD and strengthen the notion

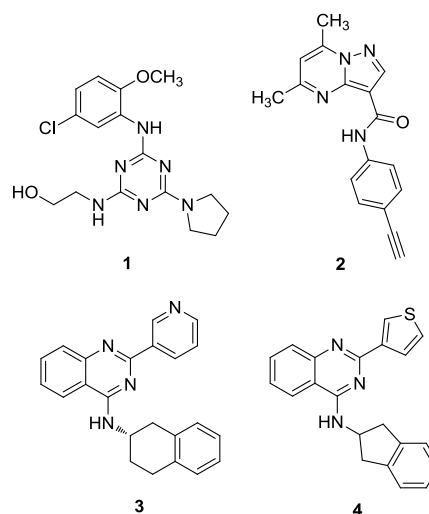


Figure 1. Structures of GCCase inhibitors and activators.

Received: August 15, 2018

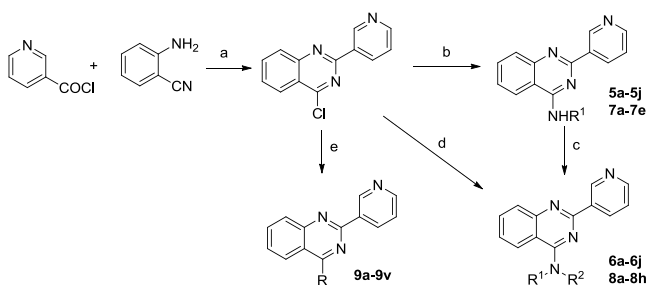
that GCase is a valuable target for the treatment of synucleinopathies.

In our previous work,¹⁹ we discovered a series of quinazoline inhibitors with nanomolar potency (see representative compounds **3** and **4**, Figure 1). Here, we unexpectedly found that N-methylation of some of the quinazoline analogues transformed quinazoline inhibitors into activators. We describe a broader structure–activity relationship (SAR) study of quinazoline derivatives to better understand the pharmacophoric requirements for this unusual activity switch as a result of such a minor structural change and to design novel noninhibitory modulators.

CHEMISTRY

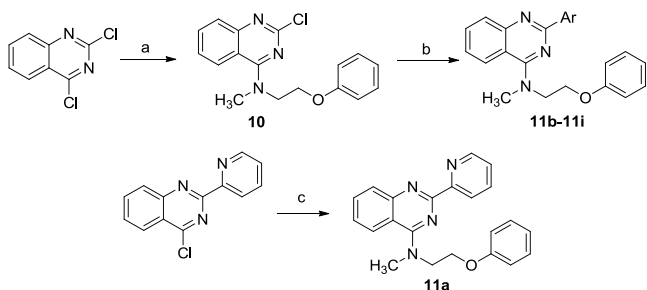
The synthesis of target compounds for SAR exploration is similar to our previous synthesis route¹⁹ and is detailed in Schemes 1 and 2. As shown in Scheme 1, the intermediate 4-

Scheme 1. Synthesis of N-Methyl Quinazoline Derivatives^a



^aReagents and conditions: (a) (i) sulfolane (ii) PCl_5 ; 46%; (b) R^1NH_2 , K_2CO_3 , DMF; 34–73%; (c) (i) NaH, DMF (ii) R^2I ; (d) $\text{R}^1\text{R}^2\text{NH}$, K_2CO_3 , DMF; 33–96%; (e) RH, K_2CO_3 , DMF; 26–89%.

Scheme 2. Synthesis of 11a–11i with Modifications at the 2-Position of the Quinazoline Ring^a



^aReagents and conditions: (a) N-methyl-2-phenoxyethanamine, K_2CO_3 , DMF, 80%; (b) ArB(OH)_2 , $\text{Pd(PPh}_3)_4$, K_2CO_3 , 1,4-dioxane, H_2O ; 40–82%; (c) N-methyl-2-phenoxyethanamine, K_2CO_3 , DMF, 73%.

chloro-2-(pyridin-3-yl)quinazoline was prepared from 2-amino-benzonitrile and nicotinoyl chloride according to a published synthesis route.²⁰ The reaction of 4-chloro-2-(pyridin-3-yl)quinazoline and appropriate amines in the presence of potassium carbonate as a base afforded **5a–5j** and **7a–7e**. Compounds **6a–6j**, **8a–8h**, and **9a–9v** were obtained either by deprotonation and N-methylation of the corresponding secondary amines (**5a–5j** and **7a–7e**), or by alkylation of 4-chloro-2-(pyridin-3-yl)quinazoline with appropriate secondary amines under basic conditions.

Additional analogues, having modifications at position 2 of the quinazoline ring, were synthesized by reaction of N-methyl-

2-phenoxyethanamine with 2,4-dichloroquinazoline, followed by Suzuki coupling with appropriate boronic acids to afford **11b–11i** (Scheme 2). Compound **11a** was synthesized by reaction of commercially available 4-chloro-2-(pyridin-2-yl)quinazoline and N-methyl-2-phenoxyethanamine. The structure and purity of all of the prepared compounds were confirmed by spectroscopic and analytical techniques.

RESULTS AND DISCUSSION

Because of our unexpected observation that N-methylation of inhibitor **5a** to **6a** ($\text{R}^2 = \text{CH}_3$) transformed its activity into an activator (Figure 2), we explored a broader SAR of quinazoline derivatives in an attempt to uncover the pharmacophoric basis for this finding and to identify novel noninhibitory modulators. First, we examined a series of moderate to potent quinazoline inhibitors that we previously reported¹⁹ to see if they could also be switched to activators by N-methylation (Table 1). Interestingly, we were able to switch the moderately active inhibitors (**5a–5f**) to activators (**6a–6f**) by N-methylation, suggesting that these inhibitors and activators may share an allosteric binding site. According to our recent findings, the N–H forms a H-bond with Ser345 in the allosteric site;²¹ this interaction may be important for attaining an inhibitory conformation, and N-methylation disrupted the H-bond and may change that conformation to one that promotes activation.

However, for the most potent inhibitors (**5g–5j**), N-methylation only produced weak inhibitory or inactive compounds (**6g–6j**). As we noted in our inhibitor SAR study,²⁰ the most potent inhibitors (**5h–5j**), having fused substituents (R groups), have additional hydrophobic interactions (and π – π stacking with Phe347) with loop 2 residues of GCase, which stabilizes the GCase dimer form. The removal of this presumed NH H-bond interaction with Ser345 is apparently not sufficient to completely change the conformation and/or break dimer formation so that these compounds retain partial inhibitory activity, and are not activators. Therefore, substituents of the secondary amines of inhibitors might also affect an activity switch.

To further explore the SAR, a methylene group in the phenylpropyl substituent of **5a** was modified to an oxygen atom to give ether **7a**, which was a moderate activator even without N-methylation (Figure 3). Compared to **7a**, the compounds with a longer substituent (**7b** and **7c**) or with a methyl group at the α - or β -position of **7a** (**7d** and **7e**) retained their inhibitory activity (Table 2). This finding suggests that the oxygen atom in **7a** may be involved in an intramolecular H-bond interaction with the NH group to avoid the intermolecular H-bond with Ser345, but an appropriate distance between the oxygen atom and quinazoline ring with no steric hindrance was required for proper H-bonding and to achieve this activation. Installation of an N-methyl group on the secondary amine of **7a** afforded **8a**, having the greatest maximum activation (E_{max} 761%) with an AC_{50} value (3.55 μM) similar to that of **7a** (Figure 3). Likewise, N-methylation of **7b–7e** switched these inhibitors to moderate activators **8b–8e** (Table 2). Activation of **8f–8h** was decreased with a longer substituent or with increased steric hindrance of the carbon substituents (Table 2), suggesting a small hydrophobic pocket for the alkyl groups.

To further explore the conformation required for the activation activity, some conformationally restricted substituents were introduced in the modulators (**9a–9k**, Table 3). As we expected, these compounds, without a free NH group,

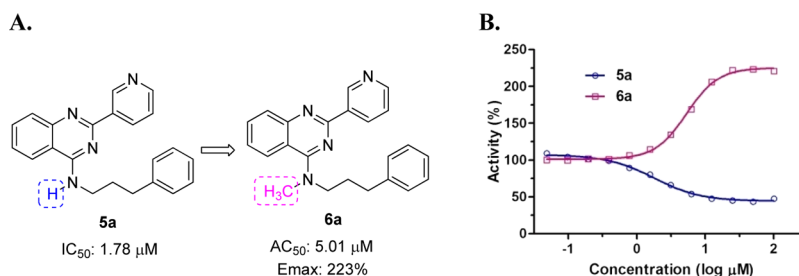
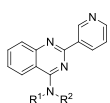


Figure 2. GCCase enzyme activity switch by N-methylation of quinazoline derivatives. (A) Example of the change in activity by N-methylation; (B) plot demonstrating the change in activity from inhibition (5a) to activation (6a).

Table 1. Structure and Enzyme Activity of Quinazoline Derivatives without and with the N-Methyl Substituent^a



Cmpd	R ¹	R ²	IC ₅₀ (μM)	AC ₅₀ (μM)	E _{max} (%)
5a		H	1.78 ± 0.22		
6a		CH ₃		5.01 ± 0.24	223
5b		H	0.097 ± 0.009		
6b		CH ₃		1.39 ± 0.26	126
5c		H	1.28 ± 0.13		
6c		CH ₃		3.99 ± 0.17	190
5d		H	0.72 ± 0.05		
6d		CH ₃		6.36 ± 0.36	149
5e		H	0.177 ± 0.012		
6e		CH ₃		2.36 ± 0.69	137
5f		H	0.042 ± 0.003		
6f		CH ₃		9.94 ± 0.38	
5g		H	0.027 ± 0.002		
6g		CH ₃		8.38 ± 0.70	
5h		H	0.0083 ± 0.001		
6h		CH ₃		2.14 ± 0.24	
5i		H	0.0087 ± 0.0011		
6i		CH ₃		0.43 ± 0.02	
5j		H	0.0099 ± 0.0013		
6j		CH ₃		5.87 ± 0.24	

^aExperiments were performed in triplicate, and the mean ± SD is shown.

displayed activation activity (except for 9g and 9h). Interestingly, the chiral center of the stereoisomers (9b and 9c) did not have a striking effect on the activity. We had previously demonstrated the important role of an aromatic ring in the N-substituents of our quinazoline inhibitors;¹⁹ here, we

also observed the key interaction of the aromatic ring in the activators. For example, compared to 9j, compound 9k with a fused phenyl ring gave a 5-fold lower AC₅₀ value.

To pursue potent activators with greater maximum activation, we further designed and synthesized derivatives 9l–9v having a conformationally restricted chain or a fused ring (Table 3). Most of the compounds showed similar activation activity as 8a, except for 9n, 9u, and 9v. Similar to 9b and 9c, compound 9q has slightly better binding potency than its enantiomer (9r).

Finally, we examined the aromatic ring effect at position 2 of the quinazoline ring (Table 4). As we found in our SAR of quinazoline inhibitors, the 3-pyridinyl ring could be replaced by other aromatic rings, such as phenyl and 3-thienyl groups, without losing activity.¹⁹ Unlike the inhibitors, the activator series modulators were not tolerant of modification of the 3-pyridinyl ring, except for 11b, 11c, and 11h, which were comparable or enhanced in activity relative to 8a. It should be noted that compound binding to the GCCase allosteric site may not induce either inhibitory or activation activity because the readout of compound activity was based on the enzyme activity. A binding affinity-based or competitive-binding assay may be developed for accurate evaluation of the compounds without inhibitory or activation activity.

To verify compound activity in cells, the most active compounds underwent preliminary screening in healthy control fibroblast cell assays. Compound 9q, showing the most promising effect, was further tested in healthy control and compound heterozygous N370S/84GG *GBA1* mutant fibroblasts derived from a GD patient. Compound treatment increased the post-ER form (resistant to Endo H digestion) of wild-type GCCase protein levels and improved enzyme activity at a concentration of 15 μM in control fibroblasts, while control compound isofagomine (IFG) did not change post-ER GCCase levels and enzyme activity at a concentration of 25 μM (Figures 4A and 5A). Similarly, we observed an increase of GCCase protein levels and improved enzyme activity upon 9q treatment in N370S/84GG *GBA1* mutant fibroblasts (Figures 4B and 5B).

To confirm that the increase of GCCase activity observed in fibroblast lysates occurred because of an increase in lysosomal GCCase, we measured GCCase activity in live cells. Fibroblasts from a healthy control and fibroblasts containing a homozygous N370S or L444P *GBA1* mutation were treated with 9q and IFG and assayed for lysosomal GCCase activity. Lysosomal specificity was achieved by calculating only the bafilomycin-sensitive hydrolysis of the substrate. We found that treatment with 9q led to a significant, dose-dependent, increase in lysosomal GCCase activity in healthy control and *GBA1* mutant fibroblasts with a 55 and 85% increase in the 15 μM

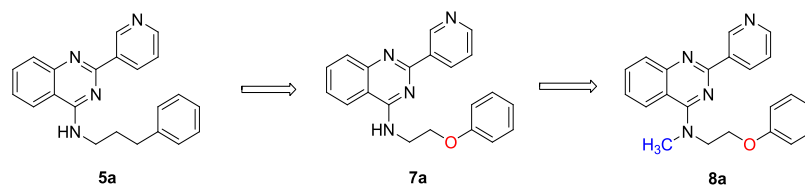


Figure 3. Modification of the N-substituent by oxygen replacement (7a) and N-methylation (8a).

Table 2. Structures and Inhibition or Activation Activity of Quinazoline Derivatives Having an Oxygen Isostere and Methylation in the N-Substituent^a

Cmpd	R ¹	R ²	IC ₅₀ (μM)	AC ₅₀ (μM)	E _{max} (%)
7a		H		1.56 ± 0.30	140
8a		CH ₃		3.55 ± 0.23	761
7b		H	7.30 ± 0.33		
8b		CH ₃		16.87 ± 0.27	394
7c		H	2.54 ± 0.12		
8c		CH ₃		6.16 ± 0.15	208
7d		H	4.24 ± 0.25		
8d		CH ₃		8.97 ± 0.41	390
7e		H	1.88 ± 0.21		
8e		CH ₃		7.52 ± 0.42	345
8f		CH ₂ CH ₃		5.38 ± 0.34	478
8g		CH ₂ CH ₂ CH ₃		3.18 ± 0.69	132
8h					Inactive

^aExperiments were performed in triplicate, and the mean ± SD is shown.

treated N370S and L444P fibroblast, respectively (Figure 5C–E). In contrast, treatment with IFG showed little or no effect on GCase activity.

Similar effects were observed in induced pluripotent stem cell (iPSC)-derived healthy control neurons and heterozygous N370S *GBA1* mutant dopaminergic neurons from a PD patient (see Supporting Information Figure for the characterization of iPSCs and differentiated neurons) treated with increasing concentrations of 9q for 10 days and digested with Endo H or PNGase. 9q increased GCase protein levels and enzyme activity in both wild-type and mutant neurons (Figures 6 and 7), suggesting the potential application of these GCase modulators in PD patients with/without *GBA1* mutations.

CONCLUSIONS

Our SAR study revealed a remarkable finding that previously reported quinazoline inhibitors could be transformed to

activators of GCase by N-methylation. Treatment of wild-type and *GBA1* mutant fibroblasts, as well as dopaminergic neurons with modulator 9q, led to increased GCase protein levels and lysosomal enzyme activity, suggesting that further development of these compounds as GCase allosteric activators is warranted. It will be important to analyze the GCase-compound complex by crystallography to elucidate the mechanism of enzyme activation for future drug design.

EXPERIMENTAL SECTION

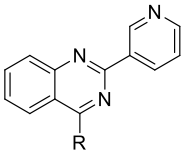
Chemistry. Materials, and Methods. Commercially available reagents and solvents were used without further purification. All reactions were monitored by thin-layer chromatography (TLC) using 0.25 mm SiliCycle extra hard 250 μM TLC plates (60 F254). Purification of reaction products was carried out by flash chromatography using an Agilent 971-FP flash purification system with SiliCycle silica gel columns. The yields are not optimized. The purity of all compounds was >95% as analyzed with an Agilent 1260 Infinity HPLC system. ¹H NMR and ¹³C NMR spectra were obtained using a Bruker AVANCE III 500 MHz system (500 MHz for ¹H NMR and 125 MHz for ¹³C NMR) or Agilent DD MR-400 system (400 MHz for ¹H NMR and 100 MHz for ¹³C NMR) spectrometer. Chemical shifts are reported relative to chloroform (δ = 7.26 for ¹H NMR and δ = 77.16 for ¹³C NMR spectra) or dimethyl sulfoxide (DMSO) (δ = 2.50 for ¹H and δ = 39.52 for ¹³C NMR spectra). Data are reported as br = broad, s = singlet, d = doublet, t = triplet, q = quartet, m = multiplet. Mass spectra were obtained using a Bruker AmaZon SL system. High-resolution mass spectra (HRMS) were performed using an Agilent 6210A LC-time of flight (TOF) instrument with a dual spray electrospray ionization (ESI) source with a high resolution TOF mass analyzer and collecting in a 2 GHz detector mode coupled with an Agilent 1200 HPLC.

General Procedure for Compounds 5a–5j, 7a–7e, 9a–9v, and 11a. A mixture of 4-chloro-2-(pyridin-3-yl)quinazolin-4-amine^{19,22} (72 mg, 0.3 mmol), amine (0.3 mmol), and potassium carbonate (69 mg, 0.3 mmol) in dimethylformamide (DMF, 2 mL) was stirred at room temperature or 60 °C overnight. Water (20 mL) was added, and the formed solid was filtered, washed with water, and dried in vacuo to give the products, which were usually pure (>95% purity). Those products without sufficient purity were further purified by flash chromatography.

General Procedure for Compounds 6a–6j and 8a–8h. To a solution of 5a–5j in dry DMF was added NaH (60% in mineral oil) under an argon atmosphere at room temperature, and the mixture was stirred for 15 min. Iodomethane or an appropriate halogenated alkane was added dropwise to the mixture, and the mixture was allowed to stir at room temperature overnight. Water was added, and the formed solid was filtered, washed with water, and dried in vacuo to give the desired product.

Preparation of 2-Chloro-N-methyl-N-(2-phenoxyethyl)-quinazolin-4-amine (10). A mixture of 2,4-dichloroquinazolin-4-amine (1.99 g, 10 mmol), N-methyl-2-phenoxyethanamine (1.51 g, 10 mmol), and potassium carbonate (1.38 g, 10 mmol) in DMF (20 mL) were stirred at room temperature overnight. Water (120 mL) was added, and the formed solid was filtered, washed with water, and dried to give 10 as a white solid (2.5 g, 80%).

¹H NMR (500 MHz, CDCl₃): δ 8.10 (d, J = 8.5 Hz, 1H), 7.77 (dd, J = 8.4, 0.8 Hz, 1H), 7.71–7.65 (m, 1H), 7.37 (ddd, J = 8.4, 7.0, 1.3 Hz, 1H), 7.30–7.25 (m, 2H), 6.97–6.91 (m, 3H), 4.38 (t, J = 5.5 Hz,

Table 3. Structure and Activation Activity of Quinazoline Derivatives with Conformationally Restricted Substituents and Fused Aromatic Ring Substituents^a


Cmpd	R	AC ₅₀ (μM)	E _{max} (%)	Cmpd	R	AC ₅₀ (μM)	E _{max} (%)
9a		1.17 ± 0.09	276	9l		3.80 ± 0.03	155
9b		4.75 ± 0.09	237	9m		1.84 ± 0.08	337
9c		3.65 ± 0.34	302	9n		14.91 ± 0.95	428
9d		4.47 ± 0.37	364	9o		1.63 ± 0.13	160
9e		5.18 ± 0.08	160	9p		4.88 ± 0.29	488
9f		4.66 ± 0.22	130	9q		1.49 ± 0.06	780
9g		2.23 ± 0.13 ^b		9r		2.37 ± 0.14	296
9h		Inactive		9s		1.63 ± 0.02	674
9i		4.27 ± 0.17	175	9t		6.90 ± 0.94	517
9j		44.14 ± 4.49	423	9u		7.92 ± 1.64	197
9k		9.74 ± 1.10	438	9v		16.07 ± 0.56	643

^aExperiments were performed in triplicate, and the mean ± SD is shown. ^bInhibitor.

2H), 4.18 (t, *J* = 5.4 Hz, 2H), 3.61 (s, 3H). ¹³C NMR (125 MHz, CDCl₃): δ 163.7, 158.3, 156.1, 153.6, 133.0, 129.6, 127.8, 125.7, 124.8, 121.1, 114.4, 65.5, 52.6, 42.2. MS (ESI) *m/z*: [M + H]⁺ calcd, 314.11; found, 314.49.

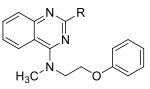
General Procedure for Compounds 11b–11h. A mixture of 2-chloro-*N*-methyl-*N*-(2-phenoxyethyl)quinazolin-4-amine (**10**, 126 mg, 0.4 mmol), boronic acid (0.5 mmol), Pd(PPh₃)₄ (50 mg, 0.05 mmol), potassium carbonate (276 mg, 2.0 mmol) in dioxane (10 mL), and water (1.5 mL) was heated at 100 °C under an argon atmosphere for 16 h. Water (5 mL) was added, and the mixture was extracted with EtOAc (25 mL × 3). The combined organic phase was washed with brine (15 mL), dried (Na₂SO₄), filtered, evaporated, and purified by flash chromatography to give the product.

Analytical Data of the Novel Quinazoline Derivatives (6a–6j, 7a–7e, 8a–8h, 9a–9v, and 11a–11h). *N*-Methyl-*N*-(3-phenylpropyl)-2-(pyridin-3-yl)quinazolin-4-amine (**6a**). Yellow solid (yield: 72%). ¹H NMR (500 MHz, CDCl₃): δ 9.69 (s, 1H), 8.70 (dt, *J* = 7.9,

1.7 Hz, 1H), 8.66 (d, *J* = 4.4 Hz, 1H), 7.92–7.84 (m, 2H), 7.71–7.63 (m, 1H), 7.37 (dd, *J* = 7.9, 4.8 Hz, 1H), 7.31–7.25 (m, 3H), 7.21–7.16 (m, 3H), 3.86–3.80 (m, 2H), 3.41 (s, 3H), 2.74 (t, *J* = 7.5 Hz, 2H), 2.25–2.16 (m, 2H). ¹³C NMR (125 MHz, CDCl₃): δ 163.3, 157.3, 152.9, 150.6, 150.2, 141.2, 135.5, 134.3, 132.1, 128.7, 128.5, 128.4, 126.1, 125.2, 124.4, 123.1, 115.0, 52.7, 40.0, 33.3, 28.8. HRMS (ESI): calcd for C₂₃H₂₃N₄ [M + H]⁺, 355.1917; found, 355.1928.

N-Methyl-*N*-phenethyl-2-(pyridin-3-yl)quinazolin-4-amine (**6b**). Pale-yellow solid (yield: 81%). ¹H NMR (500 MHz, CDCl₃): δ 9.74 (s, 1H), 8.80–8.56 (m, 2H), 7.94 (d, *J* = 8.2 Hz, 1H), 7.89 (d, *J* = 8.3 Hz, 1H), 7.70–7.62 (m, 1H), 7.41–7.30 (m, 2H), 7.30–7.16 (m, 5H), 4.07–3.97 (m, 2H), 3.39 (s, 3H), 3.17–3.07 (m, 2H). ¹³C NMR (125 MHz, CDCl₃): δ 163.0, 157.4, 152.9, 150.6, 150.1, 138.9, 135.6, 134.5, 132.2, 128.8, 128.7, 128.7, 126.5, 125.3, 124.5, 123.2, 115.0, 54.9, 40.7, 33.6. HRMS (ESI): calcd for C₂₂H₂₁N₄ [M + H]⁺, 341.1761; found, 341.1770.

Table 4. Structure and Activation Activity of *N*-Methyl-*N*-(2-phenoxyethyl)quinazolin-4-amine Derivatives Containing Aromatic Rings (11a–11g)^a



Cmpd	R	AC ₅₀ (μM)	E _{max} (%)
8a		2.30 ± 0.23	552
11a		> 50	
11b		2.89 ± 0.34	690
11c		0.89 ± 0.01	634
11d		Inactive	
11e		Inactive	
11f		Inactive	
11g		21.73 ± 7.67	229
11h		1.68 ± 0.09	145

^aExperiments were performed in triplicate, and the mean ± SD is shown.

N-Methyl-*N*-(4-phenylbutyl)-2-(pyridin-3-yl)quinazolin-4-amine (**6c**). Pale-yellow oil (yield: 67%). ¹H NMR (500 MHz, CDCl₃): δ 9.72 (s, 1H), 8.75 (d, *J* = 7.9 Hz, 1H), 8.68 (s, 1H), 7.94 (d, *J* = 7.7 Hz, 1H), 7.91 (d, *J* = 8.3 Hz, 1H), 7.71–7.66 (m, 1H), 7.42–7.33 (m, 2H), 7.28–7.23 (t, *J* = 7.6 Hz, 2H), 7.19–7.12 (m, 3H), 3.85–3.79 (m, 2H), 3.39 (s, 3H), 2.68 (t, *J* = 7.6 Hz, 2H), 1.93–1.84 (m, 2H),

1.78–1.70 (m, 2H). ¹³C NMR (125 MHz, CDCl₃): δ 163.3, 157.4, 152.9, 150.5, 150.1, 141.9, 135.6, 134.4, 132.2, 128.7, 128.3, 125.9, 125.3, 124.4, 123.3, 115.1, 53.1, 40.0, 35.6, 28.7, 26.9. HRMS (ESI): calcd for C₂₄H₂₅N₄ [M + H]⁺, 369.2074; found, 369.2080.

N-Cyclopentyl-*N*-methyl-2-(pyridin-3-yl)quinazolin-4-amine (**6d**). Yellow solid (yield: 76%). ¹H NMR (500 MHz, CDCl₃): δ 9.71 (s, 1H), 8.77 (dt, *J* = 7.9, 1.8 Hz, 1H), 8.65 (dd, *J* = 4.7, 1.5 Hz, 1H), 7.98 (d, *J* = 8.3 Hz, 1H), 7.90 (d, *J* = 8.3 Hz, 1H), 7.68 (t, *J* = 7.1 Hz, 1H), 7.44–7.31 (m, 2H), 5.04–4.92 (m, 1H), 3.25 (s, 3H), 2.15–2.02 (m, 2H), 1.86–1.60 (m, 6H). ¹³C NMR (125 MHz, CDCl₃): δ 164.4, 157.4, 152.9, 150.5, 150.2, 135.6, 134.4, 132.1, 128.6, 125.4, 124.4, 123.1, 115.5, 61.6, 34.4, 28.8, 24.6. HRMS (ESI): calcd for C₁₉H₂₁N₄ [M + H]⁺, 305.1761; found, 305.1762.

N-Cyclohexyl-*N*-methyl-2-(pyridin-3-yl)quinazolin-4-amine (**6e**). Pale-yellow solid (yield: 59%). ¹H NMR (500 MHz, CDCl₃): δ 9.72 (s, 1H), 8.79 (d, *J* = 7.8 Hz, 1H), 8.67 (d, *J* = 3.8 Hz, 1H), 7.94 (d, *J* = 8.3 Hz, 2H), 7.70 (t, *J* = 7.6 Hz, 1H), 7.43–7.33 (m, 2H), 4.58–4.46 (m, 1H), 3.28 (s, 3H), 2.01 (d, *J* = 11.5 Hz, 2H), 1.92 (d, *J* = 13.2 Hz, 2H), 1.79–1.63 (m, 3H), 1.53–1.41 (m, 2H), 1.26–1.15 (m, 1H). ¹³C NMR (125 MHz, CDCl₃): δ 163.8, 157.3, 153.0, 150.7, 150.3, 135.7, 134.4, 132.2, 128.7, 125.5, 124.4, 123.2, 115.4, 59.9, 34.3, 30.1, 26.0, 25.8. HRMS (ESI): calcd for C₂₀H₂₃N₄ [M + H]⁺, 319.1917; found, 319.1921.

N-Cycloheptyl-*N*-methyl-2-(pyridin-3-yl)quinazolin-4-amine (**6f**). Pale-yellow solid (yield: 72%). ¹H NMR (500 MHz, CDCl₃): δ 9.71 (s, 1H), 8.77 (d, *J* = 7.9 Hz, 1H), 8.65 (d, *J* = 3.5 Hz, 1H), 7.94 (d, *J* = 8.3 Hz, 1H), 7.90 (d, *J* = 8.3 Hz, 1H), 7.73–7.60 (m, 1H), 7.44–7.31 (m, 2H), 4.77–4.65 (m, 1H), 3.27 (s, 3H), 2.13–2.02 (m, 2H), 1.93–1.74 (m, 4H), 1.74–1.52 (m, 6H). ¹³C NMR (125 MHz, CDCl₃): δ 163.4, 157.4, 153.0, 150.5, 150.2, 135.6, 134.5, 132.0, 128.6, 125.4, 124.2, 123.1, 115.3, 61.2, 34.5, 32.2, 27.7, 25.5. HRMS (ESI): calcd for C₂₁H₂₅N₄ [M + H]⁺, 333.2074; found, 333.2082.

N-Cyclooctyl-*N*-methyl-2-(pyridin-3-yl)quinazolin-4-amine (**6g**). Yellow solid (yield: 86%). ¹H NMR (500 MHz, CDCl₃): δ 9.71 (d, *J* = 1.6 Hz, 1H), 8.77 (dt, *J* = 7.9, 1.9 Hz, 1H), 8.65 (dd, *J* = 4.7, 1.6 Hz, 1H), 7.96 (d, *J* = 8.4 Hz, 1H), 7.89 (d, *J* = 8.3 Hz, 1H), 7.72–7.63 (m, 1H), 7.41–7.31 (m, 2H), 4.99–4.87 (m, 1H), 3.27 (s, 3H),

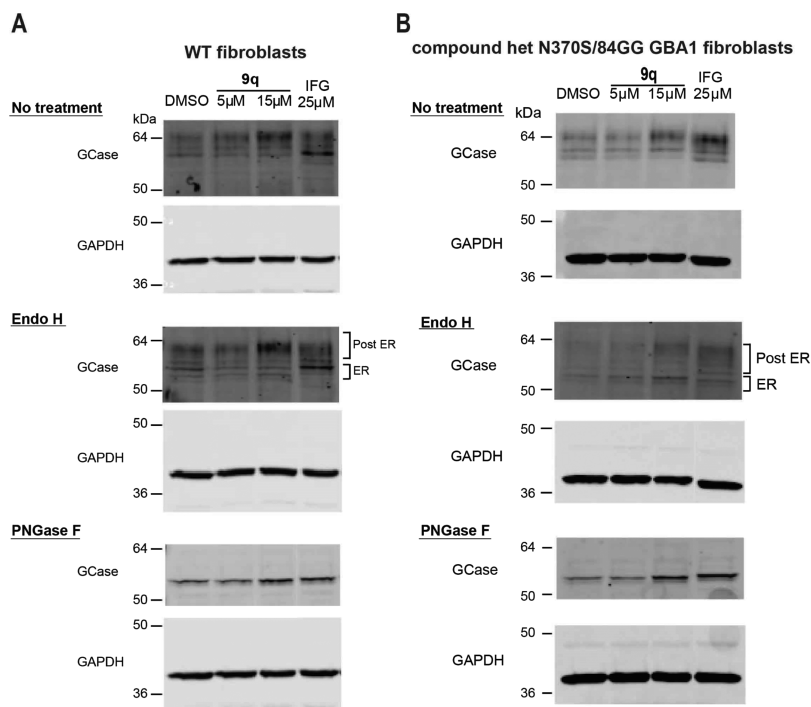


Figure 4. Activator **9q** increases GCCase protein levels in (A) healthy control fibroblasts and (B) compound heterozygous *GBA1* mutant fibroblasts (N370S/84GG) derived from a GD patient. Cell lysates from fibroblasts treated with vehicle (DMSO), **9q** (5, 15 μM), or IFG were analyzed by immunoblotting after no digestion (top), Endo H digestion (middle), and PNGase F digestion (bottom); *n* = 4.

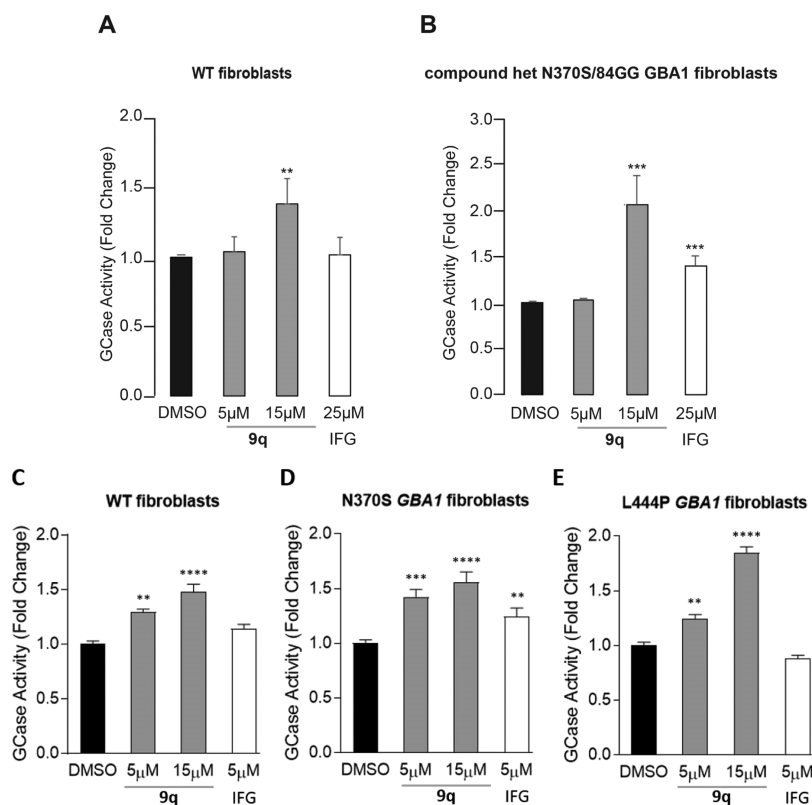


Figure 5. GCCase enzyme activity in cell lysates and in the lysosome of **9q**-treated cells. GCCase activity was measured in lysates from (A) healthy control fibroblasts and (B) compound heterozygous *GBA1* mutant fibroblasts (N370S/84GG). Lysosomal GCCase was measured using a live-cell assay in (C) healthy control, (D) homozygous N370S, and (E) homozygous L444P mutant fibroblasts after 3 day treatment with **9q** (5, 15 μ M), 5 μ M IFG, or vehicle (DMSO). The data are presented as the mean \pm SEM, $n = 3-4$; * $p < 0.05$, ** $p < 0.01$, **** $p < 0.001$ vs vehicle treatments; one-way ANOVA was followed by the Tukey's multiple comparisons post hoc test.

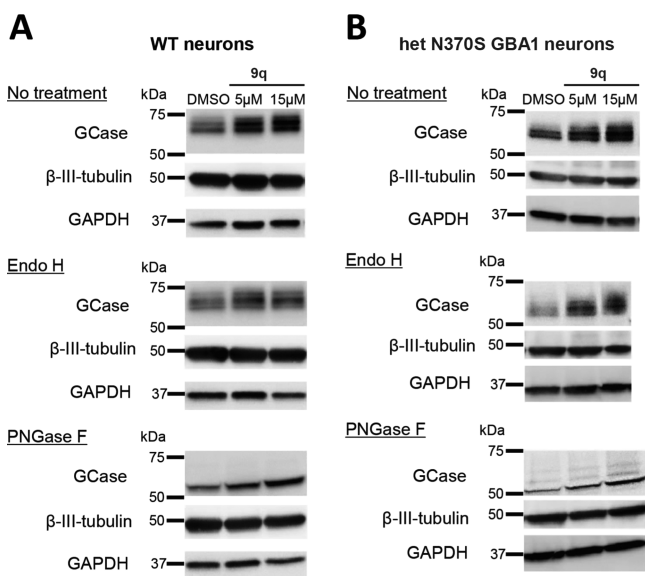


Figure 6. Activator **9q** increases GCCase protein levels and enzyme activity in (A) wild-type control and (B) patient-derived heterozygous N370S *GBA1* mutant dopaminergic neurons at day 70 of differentiation. Cell lysates from neurons treated with vehicle (DMSO) or **9q** (5, 15 μ M) for 10 consecutive days were analyzed by immunoblotting after no digestion (top), Endo H digestion (middle), and PNGase F digestion (bottom); $n = 3$.

2.02–1.87 (m, 4H), 1.87–1.77 (m, 2H), 1.77–1.52 (m, 8H). ^{13}C NMR (125 MHz, CDCl_3): δ 163.2, 157.4, 153.0, 150.5, 150.2, 135.6,

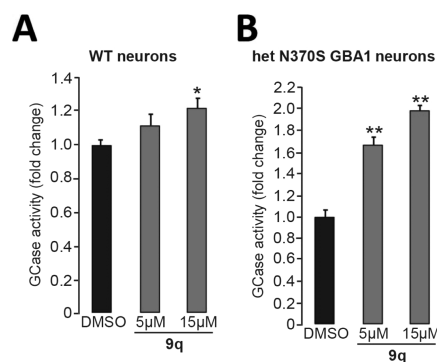


Figure 7. GCCase enzyme activity in protein lysates of (A) wild-type control and (B) patient-derived heterozygous N370S *GBA1* mutant dopaminergic neurons after 10 days consecutive treatment with vehicle (DMSO) or **9q** (day 70 of differentiation). The data are presented as the mean \pm SEM, $n = 4-7$; * $p < 0.05$, ** $p < 0.01$ versus vehicle treatments; one-way ANOVA was followed by the Tukey's multiple comparisons post hoc test.

134.5, 132.0, 128.6, 125.5, 124.2, 123.1, 115.3, 59.5, 34.7, 31.6, 29.7, 26.4, 25.2. HRMS (ESI): calcd for $\text{C}_{22}\text{H}_{27}\text{N}_4$ $[\text{M} + \text{H}]^+$, 347.2230; found, 347.2238.

N-(2,3-Dihydro-1*H*-inden-2-yl)-*N*-methyl-2-(pyridin-3-yl)-quinazolin-4-amine (**6h**). Yellow solid (yield: 60%). ^1H NMR (500 MHz, CDCl_3): δ 9.74 (d, $J = 1.5$ Hz, 1H), 8.77 (dt, $J = 7.9, 1.9$ Hz, 1H), 8.68 (dd, $J = 4.7, 1.5$ Hz, 1H), 8.04 (d, $J = 7.9$ Hz, 1H), 7.96 (d, $J = 8.3$ Hz, 1H), 7.78–7.69 (m, 1H), 7.45–7.41 (m, 1H), 7.39 (dd, $J = 7.9, 4.8$ Hz, 1H), 7.29 (dd, $J = 5.2, 3.4$ Hz, 2H), 7.25–7.20 (m, 2H), 5.66–5.58 (m, 1H), 3.47 (dd, $J = 16.4, 8.6$ Hz, 2H), 3.35–3.26 (m,

5H). ^{13}C NMR (125 MHz, CDCl_3): δ 164.7, 157.5, 153.1, 150.8, 150.4, 141.3, 135.7, 134.3, 132.5, 129.0, 126.9, 125.5, 124.8, 124.7, 123.3, 115.7, 60.2, 36.4, 35.6. HRMS (ESI): calcd for $\text{C}_{23}\text{H}_{21}\text{N}_4$ [$\text{M} + \text{H}$] $^+$, 353.1761; found, 353.1772.

(*S*)-*N*-Methyl-2-(pyridin-3-yl)-*N*-(1,2,3,4-tetrahydronaphthalen-2-yl)quinazolin-4-amine (**6i**). Pale-yellow oil (yield: 63%). ^1H NMR (500 MHz, CDCl_3): δ 9.70 (s, 1H), 8.77 (dt, $J = 7.9, 1.9$ Hz, 1H), 8.65 (s, 1H), 7.97 (d, $J = 7.7$ Hz, 1H), 7.93 (d, $J = 7.7$ Hz, 1H), 7.77–7.63 (m, 1H), 7.45–7.30 (m, 2H), 7.16–7.10 (m, 4H), 5.07–4.90 (m, 1H), 3.34 (s, 3H), 3.21 (d, $J = 8.4$ Hz, 2H), 3.12–2.91 (m, 2H), 2.29–2.17 (m, 1H), 2.11 (qd, $J = 11.9, 5.9$ Hz, 1H). ^{13}C NMR (125 MHz, CDCl_3): δ 164.1, 157.3, 153.0, 150.6, 150.2, 135.6, 135.6, 135.2, 134.3, 132.3, 129.4, 128.8, 126.1, 126.0, 125.3, 124.6, 123.2, 115.4, 56.5, 34.2, 32.0, 29.5, 27.1. HRMS (ESI): calcd for $\text{C}_{24}\text{H}_{23}\text{N}_4$ [$\text{M} + \text{H}$] $^+$, 367.1917; found, 367.1932.

(*R*)-*N*-Methyl-2-(pyridin-3-yl)-*N*-(1,2,3,4-tetrahydronaphthalen-2-yl)quinazolin-4-amine (**6j**). Pale-yellow oil (yield: 69%). ^1H NMR (500 MHz, CDCl_3): δ 9.70 (s, 1H), 8.77 (dt, $J = 7.9, 1.9$ Hz, 1H), 8.65 (s, 1H), 7.97 (d, $J = 7.7$ Hz, 1H), 7.93 (d, $J = 7.7$ Hz, 1H), 7.77–7.63 (m, 1H), 7.45–7.30 (m, 2H), 7.16–7.10 (m, 4H), 5.07–4.90 (m, 1H), 3.34 (s, 3H), 3.21 (d, $J = 8.4$ Hz, 2H), 3.12–2.91 (m, 2H), 2.29–2.17 (m, 1H), 2.11 (qd, $J = 11.9, 5.9$ Hz, 1H). ^{13}C NMR (125 MHz, CDCl_3): δ 164.1, 157.3, 153.0, 150.6, 150.2, 135.6, 135.6, 135.2, 134.3, 132.3, 129.4, 128.8, 126.1, 126.0, 125.3, 124.6, 123.2, 115.4, 56.5, 34.2, 32.0, 29.5, 27.1. HRMS (ESI): calcd for $\text{C}_{24}\text{H}_{23}\text{N}_4$ [$\text{M} + \text{H}$] $^+$, 367.1917; found, 367.1927.

N-(2-Phenoxyethyl)-2-(pyridin-3-yl)quinazolin-4-amine (**7a**). Off-white solid (yield: 67%). ^1H NMR (500 MHz, CDCl_3): δ 9.75 (d, $J = 1.6$ Hz, 1H), 8.81 (dt, $J = 7.9, 1.9$ Hz, 1H), 8.70 (dd, $J = 4.8, 1.6$ Hz, 1H), 7.93 (d, $J = 8.2$ Hz, 1H), 7.79–7.73 (m, 2H), 7.50–7.46 (m, 1H), 7.42 (dd, $J = 7.9, 4.8$ Hz, 1H), 7.34–7.28 (m, 2H), 7.01–6.95 (m, 3H), 6.28–6.17 (m, 1H), 4.39–4.29 (m, 2H), 4.28–4.23 (m, 2H). ^{13}C NMR (125 MHz, CDCl_3): δ 159.7, 158.6, 150.8, 150.4, 150.3, 135.7, 134.4, 132.9, 129.7, 129.0, 126.0, 123.3, 121.3, 120.8, 114.6, 114.0, 66.4, 40.8. HRMS (ESI): calcd for $\text{C}_{21}\text{H}_{19}\text{N}_4\text{O}$ [$\text{M} + \text{H}$] $^+$, 343.1553; found, 343.1564.

N-Methyl-*N*-(2-phenoxypropyl)-2-(pyridin-3-yl)quinazolin-4-amine (**8a**). Off-white solid (yield: 96%). ^1H NMR (500 MHz, CDCl_3): δ 9.69 (s, 1H), 8.75 (dt, $J = 7.9, 1.9$ Hz, 1H), 8.67 (d, $J = 3.5$ Hz, 1H), 8.13 (d, $J = 8.5$ Hz, 1H), 7.92 (d, $J = 8.4$ Hz, 1H), 7.71 (ddd, $J = 8.3, 7.0, 1.3$ Hz, 1H), 7.44–7.34 (m, 2H), 7.28–7.24 (m, 2H), 6.96–6.87 (m, 3H), 4.45 (t, $J = 5.4$ Hz, 2H), 4.28 (t, $J = 5.4$ Hz, 2H), 3.63 (s, 3H). ^{13}C NMR (125 MHz, CDCl_3): δ 163.1, 158.5, 157.2, 153.0, 150.7, 150.1, 135.5, 134.2, 132.3, 129.5, 128.8, 125.5, 124.6, 123.2, 121.1, 115.1, 114.5, 65.9, 52.5, 41.9. HRMS (ESI): calcd for $\text{C}_{22}\text{H}_{21}\text{N}_4\text{O}$ [$\text{M} + \text{H}$] $^+$, 357.1710; found, 357.1722.

N-(2-(Benzyloxy)ethyl)-2-(pyridin-3-yl)quinazolin-4-amine (**7b**). Pale-yellow solid (51%). ^1H NMR (500 MHz, CDCl_3): δ 9.72 (s, 1H), 8.77 (d, $J = 7.9$ Hz, 1H), 8.68 (s, 1H), 7.90 (d, $J = 8.3$ Hz, 1H), 7.78–7.71 (m, 1H), 7.68 (d, $J = 8.1$ Hz, 1H), 7.46–7.41 (m, 1H), 7.41–7.37 (m, 1H), 7.36–7.30 (m, 4H), 6.27–6.16 (m, 1H), 4.59 (s, 2H), 4.01 (q, $J = 5.2$ Hz, 2H), 3.84–3.80 (m, 2H). ^{13}C NMR (125 MHz, CDCl_3): δ 159.6, 158.5, 150.6, 150.2, 150.1, 137.8, 135.6, 132.7, 128.8, 128.5, 127.9, 127.8, 125.8, 123.2, 120.7, 113.9, 73.3, 68.4, 41.0. HRMS (ESI): calcd for $\text{C}_{22}\text{H}_{21}\text{N}_4\text{O}$ [$\text{M} + \text{H}$] $^+$, 357.1710; found, 357.1721.

N-(2-(Benzyloxy)ethyl)-*N*-methyl-2-(pyridin-3-yl)quinazolin-4-amine (**8b**). Pale-yellow oil (87%). ^1H NMR (500 MHz, CDCl_3): δ 9.63 (s, 1H), 8.68 (dt, $J = 7.9, 1.9$ Hz, 1H), 8.61 (d, $J = 3.7$ Hz, 1H), 8.07 (dd, $J = 8.4, 0.8$ Hz, 1H), 7.85 (dd, $J = 8.4, 0.8$ Hz, 1H), 7.63 (ddd, $J = 8.3, 7.0, 1.3$ Hz, 1H), 7.34–7.28 (m, 2H), 7.24–7.16 (m, 5H), 4.50 (s, 2H), 4.01 (t, $J = 5.5$ Hz, 2H), 3.88 (t, $J = 5.5$ Hz, 2H), 3.46 (s, 3H). ^{13}C NMR (125 MHz, CDCl_3): δ 163.2, 157.2, 152.9, 150.6, 150.1, 138.0, 135.5, 134.3, 132.2, 128.7, 128.4, 127.7, 127.5, 125.6, 124.5, 123.1, 115.1, 73.3, 68.1, 53.1, 41.2. HRMS (ESI): calcd for $\text{C}_{23}\text{H}_{22}\text{N}_4\text{O}$ [$\text{M} + \text{H}$] $^+$, 371.1866; found, 371.1880.

N-(3-Phenoxypropyl)-2-(pyridin-3-yl)quinazolin-4-amine (**7c**). Off-white solid (yield: 73%). ^1H NMR (500 MHz, CDCl_3): δ 9.75 (s, 1H), 8.79 (d, $J = 7.9$ Hz, 1H), 8.66 (d, $J = 3.4$ Hz, 1H), 7.89 (d, $J = 8.4$ Hz, 1H), 7.77–7.63 (m, 2H), 7.47–7.39 (m, 1H), 7.37 (dd, $J =$

7.8, 4.8 Hz, 1H), 7.32–7.25 (m, 2H), 6.99–6.90 (m, 3H), 6.50 (s, 1H), 4.18 (t, $J = 5.6$ Hz, 2H), 4.02–3.95 (m, 2H), 2.28 (p, $J = 5.9$ Hz, 2H). ^{13}C NMR (125 MHz, CDCl_3): δ 159.7, 158.6, 158.5, 150.6, 150.2, 150.2, 135.6, 134.5, 132.7, 129.6, 128.8, 125.8, 123.1, 121.1, 120.6, 114.4, 113.9, 66.8, 39.7, 28.5. HRMS (ESI): calcd for $\text{C}_{22}\text{H}_{21}\text{N}_4\text{O}$ [$\text{M} + \text{H}$] $^+$, 357.1710; found, 357.1723.

N-Methyl-*N*-(3-phenoxypropyl)-2-(pyridin-3-yl)quinazolin-4-amine (**8c**). Yellow solid (77%). ^1H NMR (500 MHz, CDCl_3): δ 9.72 (s, 1H), 8.77 (dt, $J = 7.9, 1.9$ Hz, 1H), 8.66 (d, $J = 3.7$ Hz, 1H), 8.06 (dd, $J = 8.4, 0.8$ Hz, 1H), 7.91 (dd, $J = 8.4, 0.8$ Hz, 1H), 7.70 (ddd, $J = 8.3, 7.0, 1.3$ Hz, 1H), 7.42–7.33 (m, 2H), 7.29–7.24 (m, 2H), 6.93 (t, $J = 7.3$ Hz, 1H), 6.88 (d, $J = 7.8$ Hz, 2H), 4.10 (t, $J = 5.8$ Hz, 2H), 4.07–4.02 (m, 2H), 3.48 (s, 3H), 2.40–2.32 (m, 2H). ^{13}C NMR (125 MHz, CDCl_3): δ 163.2, 158.7, 157.3, 152.9, 150.6, 150.1, 135.6, 134.3, 132.2, 129.5, 128.8, 125.4, 124.5, 123.1, 120.8, 115.1, 114.4, 65.2, 50.5, 40.5, 27.2. HRMS (ESI): calcd for $\text{C}_{23}\text{H}_{22}\text{N}_4\text{O}$ [$\text{M} + \text{H}$] $^+$, 371.1866; found, 371.1879.

N-(2-Phenoxypropyl)-2-(pyridin-3-yl)quinazolin-4-amine (**7d**). Off-white solid (yield: 34%). ^1H NMR (500 MHz, CDCl_3): δ 9.76 (s, 1H), 8.79 (d, $J = 7.9$ Hz, 1H), 8.71 (s, 1H), 7.92 (d, $J = 7.9$ Hz, 1H), 7.75 (ddd, $J = 8.3, 7.0, 1.2$ Hz, 1H), 7.69 (d, $J = 7.8$ Hz, 1H), 7.50–7.36 (m, 2H), 7.31–7.26 (m, 2H), 7.02–6.91 (m, 3H), 6.35–6.20 (m, 1H), 4.87–4.75 (m, 1H), 4.31 (ddd, $J = 13.9, 6.8, 3.5$ Hz, 1H), 3.85 (ddd, $J = 13.9, 7.5, 4.7$ Hz, 1H), 1.44 (d, $J = 6.2$ Hz, 3H). ^{13}C NMR (125 MHz, CDCl_3): δ 159.6, 158.5, 157.6, 150.7, 150.3, 150.2, 135.6, 134.3, 132.8, 129.7, 128.9, 126.0, 123.2, 121.4, 120.6, 116.2, 113.8, 72.8, 46.1, 17.6. HRMS (ESI): calcd for $\text{C}_{22}\text{H}_{21}\text{N}_4\text{O}$ [$\text{M} + \text{H}$] $^+$, 357.1710; found, 357.1720.

N-Methyl-*N*-(2-phenoxypropyl)-2-(pyridin-3-yl)quinazolin-4-amine (**8d**). Off-white solid (yield: 67%). ^1H NMR (500 MHz, CDCl_3): δ 9.67 (s, 1H), 8.74 (dt, $J = 7.9, 1.7$ Hz, 1H), 8.67 (d, $J = 3.8$ Hz, 1H), 8.04 (d, $J = 8.3$ Hz, 1H), 7.91 (d, $J = 8.2$ Hz, 1H), 7.73–7.65 (m, 1H), 7.38 (dd, $J = 7.9, 4.8$ Hz, 1H), 7.37–7.32 (m, 1H), 7.21–7.13 (m, 2H), 6.91–6.79 (m, 3H), 5.06–4.97 (m, 1H), 4.36 (dd, $J = 14.1, 3.2$ Hz, 1H), 3.90 (dd, $J = 14.1, 8.1$ Hz, 1H), 3.59 (s, 3H), 1.42 (d, $J = 6.2$ Hz, 3H). ^{13}C NMR (125 MHz, CDCl_3): δ 163.0, 157.8, 157.1, 153.0, 150.6, 150.0, 135.6, 134.3, 132.3, 129.5, 128.6, 125.6, 124.5, 123.2, 121.0, 115.7, 115.0, 72.9, 58.4, 42.9, 18.1. HRMS (ESI): calcd for $\text{C}_{23}\text{H}_{22}\text{N}_4\text{O}$ [$\text{M} + \text{H}$] $^+$, 371.1866; found, 371.1879.

N-(1-Phenoxypropan-2-yl)-2-(pyridin-3-yl)quinazolin-4-amine (**7e**). Pale-yellow solid (yield: 60%). ^1H NMR (500 MHz, CDCl_3): δ 10.01 (s, 1H), 9.08 (d, $J = 7.9$ Hz, 1H), 8.96 (s, 1H), 8.21 (d, $J = 8.2$ Hz, 1H), 8.09–7.96 (m, 2H), 7.76–7.65 (m, 2H), 7.58–7.50 (m, 3H), 7.26–7.21 (m, 2H), 6.44 (d, $J = 7.1$ Hz, 1H), 5.39–5.29 (m, 1H), 4.51 (dd, $J = 9.4, 4.3$ Hz, 1H), 4.46 (dd, $J = 9.3, 3.7$ Hz, 1H), 1.84 (d, $J = 6.8$ Hz, 3H). ^{13}C NMR (125 MHz, CDCl_3): δ 159.0, 158.6, 158.4, 150.5, 150.1, 150.0, 135.8, 134.3, 132.9, 129.6, 128.7, 126.0, 123.3, 121.3, 120.7, 114.6, 113.8, 70.3, 46.2, 17.5. HRMS (ESI): calcd for $\text{C}_{22}\text{H}_{21}\text{N}_4\text{O}$ [$\text{M} + \text{H}$] $^+$, 357.1710; found, 357.1726.

N-Methyl-*N*-(1-phenoxypropan-2-yl)-2-(pyridin-3-yl)quinazolin-4-amine (**8e**). Pale-yellow oil (yield: 78%). ^1H NMR (500 MHz, CDCl_3): δ 9.71 (s, 1H), 8.76 (d, $J = 7.9$ Hz, 1H), 8.67 (s, 1H), 8.06 (d, $J = 8.4$ Hz, 1H), 7.93 (d, $J = 8.4$ Hz, 1H), 7.73–7.66 (m, 1H), 7.43–7.32 (m, 2H), 7.22 (dd, $J = 8.6, 7.5$ Hz, 2H), 6.91 (t, $J = 7.4$ Hz, 1H), 6.84 (d, $J = 7.8$ Hz, 2H), 5.27–5.16 (m, 1H), 4.28 (dd, $J = 9.8, 7.6$ Hz, 1H), 4.16 (dd, $J = 9.9, 5.1$ Hz, 1H), 3.34 (s, 3H), 1.51 (d, $J = 6.9$ Hz, 3H). ^{13}C NMR (125 MHz, CDCl_3): δ 164.5, 158.4, 157.3, 153.0, 150.6, 150.2, 135.6, 134.3, 132.3, 129.5, 128.7, 125.4, 124.6, 123.2, 121.1, 115.4, 114.6, 69.2, 54.4, 33.9, 14.3. HRMS (ESI): calcd for $\text{C}_{23}\text{H}_{22}\text{N}_4\text{O}$ [$\text{M} + \text{H}$] $^+$, 371.1866; found, 371.1882.

N-Ethyl-*N*-(2-phenoxyethyl)-2-(pyridin-3-yl)quinazolin-4-amine (**8f**). Off-white solid (yield: 68%). ^1H NMR (500 MHz, CDCl_3): δ 9.69 (d, $J = 1.5$ Hz, 1H), 8.74 (dt, $J = 7.9, 1.9$ Hz, 1H), 8.67 (dd, $J = 4.8, 1.6$ Hz, 1H), 8.00 (d, $J = 8.4$ Hz, 1H), 7.93 (d, $J = 8.4$ Hz, 1H), 7.74–7.67 (m, 1H), 7.43–7.34 (m, 2H), 7.26–7.22 (m, 2H), 6.95–6.87 (m, 3H), 4.42 (t, $J = 5.6$ Hz, 2H), 4.21 (t, $J = 5.6$ Hz, 2H), 3.94 (q, $J = 7.1$ Hz, 2H), 1.53 (t, $J = 7.1$ Hz, 3H). ^{13}C NMR (125 MHz, CDCl_3): δ 162.8, 158.5, 157.2, 152.9, 150.7, 150.1, 135.5, 134.2, 132.3, 129.5, 129.0, 124.9, 124.8, 123.2, 121.0, 115.2, 114.5, 65.7,

49.7, 47.7, 13.7. HRMS (ESI): calcd for $C_{23}H_{22}N_4O$ [M + H]⁺, 371.1866; found, 371.1882.

N-(2-Phenoxyethyl)-N-propyl-2-(pyridin-3-yl)quinazolin-4-amine (8g). Pale-yellow solid (yield: 49%). ¹H NMR (500 MHz, CDCl₃): δ 9.68 (d, J = 1.7 Hz, 1H), 8.74 (dt, J = 7.9, 1.7 Hz, 1H), 8.66 (dd, J = 4.8, 1.5 Hz, 1H), 7.97 (d, J = 8.4 Hz, 1H), 7.93 (d, J = 8.3 Hz, 1H), 7.74–7.66 (m, 1H), 7.43–7.35 (m, 2H), 7.27–7.21 (m, 2H), 6.95–6.87 (m, 3H), 4.41 (t, J = 5.6 Hz, 2H), 4.22 (t, J = 5.6 Hz, 2H), 3.84–3.78 (m, 2H), 2.02–1.93 (m, 2H), 1.02 (t, J = 7.4 Hz, 3H). ¹³C NMR (125 MHz, CDCl₃): δ 162.9, 158.5, 157.2, 152.9, 150.7, 150.1, 135.5, 134.2, 132.3, 129.5, 129.0, 124.9, 124.7, 123.2, 121.0, 115.2, 114.5, 65.7, 54.8, 50.4, 21.6, 11.3. HRMS (ESI): calcd for $C_{24}H_{25}N_4O$ [M + H]⁺, 385.2023; found, 385.2039.

N-(Cyclopropylmethyl)-N-(2-phenoxyethyl)-2-(pyridin-3-yl)quinazolin-4-amine (8h). Off-white solid (33%). ¹H NMR (500 MHz, CDCl₃): δ 9.70 (d, J = 1.5 Hz, 1H), 8.75 (dt, J = 7.9, 1.8 Hz, 1H), 8.67 (dd, J = 4.7, 1.4 Hz, 1H), 8.10 (d, J = 8.4 Hz, 1H), 7.93 (d, J = 8.4 Hz, 1H), 7.78–7.65 (m, 1H), 7.45–7.34 (m, 2H), 7.23 (t, J = 15.9 Hz, 2H), 6.92 (t, J = 7.3 Hz, 1H), 6.88 (d, J = 8.0 Hz, 2H), 4.43 (t, J = 5.6 Hz, 2H), 4.34 (t, J = 5.6 Hz, 2H), 3.79 (d, J = 6.3 Hz, 2H), 1.36–1.26 (m, 1H), 0.70–0.63 (m, 2H), 0.38–0.32 (m, 2H). ¹³C NMR (125 MHz, CDCl₃): δ 163.3, 158.5, 157.2, 152.9, 150.7, 150.1, 135.6, 134.2, 132.3, 129.5, 129.0, 125.1, 124.9, 123.2, 121.0, 115.3, 114.5, 65.9, 57.2, 49.6, 10.1, 4.0. HRMS (ESI): calcd for $C_{25}H_{25}N_4O$ [M + H]⁺, 397.2023; found, 397.2043.

4-(3-Phenoxypropyl)-2-(pyridin-3-yl)quinazolin-4-amine (9a). Pale-yellow solid (yield: 31%). ¹H NMR (500 MHz, CDCl₃): δ 9.71 (d, J = 1.5 Hz, 1H), 8.76 (dt, J = 7.9, 1.9 Hz, 1H), 8.65 (dd, J = 4.8, 1.7 Hz, 1H), 8.17 (d, J = 8.3 Hz, 1H), 7.91 (dd, J = 8.3, 0.7 Hz, 1H), 7.72–7.67 (m, 1H), 7.41–7.35 (m, 2H), 7.33–7.28 (m, 2H), 6.98 (t, J = 7.4 Hz, 1H), 6.93 (d, J = 7.9 Hz, 2H), 5.09–5.13 (m, 1H), 4.39–4.27 (m, 2H), 4.27–4.14 (m, 2H), 2.54–2.40 (m, 1H), 2.33–2.17 (m, 1H). ¹³C NMR (125 MHz, CDCl₃): δ 160.0, 157.8, 156.9, 152.5, 150.6, 150.2, 135.5, 134.3, 132.2, 129.7, 128.6, 125.1, 124.6, 123.0, 121.4, 115.6, 115.3, 75.1, 55.9, 48.8, 31.4. HRMS (ESI): calcd for $C_{23}H_{21}N_4O$ [M + H]⁺, 369.1710; found, 369.1727.

(S)-4-(3-Phenoxypropyl)-2-(pyridin-3-yl)quinazolin-4-amine (9b). Yellow oil (yield: 79%). ¹H NMR (500 MHz, CDCl₃): δ 9.71 (d, J = 1.4 Hz, 1H), 8.73 (dt, J = 7.9, 1.9 Hz, 1H), 8.68 (dd, J = 4.8, 1.7 Hz, 1H), 7.94 (s, 1H), 7.70 (ddd, J = 8.3, 7.0, 1.3 Hz, 1H), 7.42–7.33 (m, 2H), 7.30–7.25 (m, 2H), 6.98–6.92 (m, 3H), 4.64–4.55 (m, 1H), 4.36 (dd, J = 13.1, 3.2 Hz, 1H), 4.04–3.95 (m, 1H), 3.76–3.61 (m, 2H), 2.24–2.16 (m, 1H), 2.13–2.04 (m, 1H), 1.97–1.88 (m, 1H), 1.84–1.73 (m, 2H). ¹³C NMR (125 MHz, CDCl₃): δ 165.0, 157.7, 157.2, 152.7, 150.7, 150.2, 135.6, 134.2, 132.6, 129.6, 128.9, 125.2, 125.0, 123.1, 121.3, 116.0, 115.4, 71.4, 53.4, 50.3, 30.1, 22.9. HRMS (ESI): calcd for $C_{24}H_{23}N_4O$ [M + H]⁺, 383.1866; found, 383.1881.

(R)-4-(3-Phenoxypropyl)-2-(pyridin-3-yl)quinazolin-4-amine (9c). Yellow oil (yield: 63%). ¹H NMR (500 MHz, CDCl₃): δ 9.71 (d, J = 1.4 Hz, 1H), 8.73 (dt, J = 7.9, 1.9 Hz, 1H), 8.68 (dd, J = 4.8, 1.7 Hz, 1H), 7.94 (s, 1H), 7.70 (ddd, J = 8.3, 7.0, 1.3 Hz, 1H), 7.42–7.33 (m, 2H), 7.30–7.25 (m, 2H), 6.98–6.92 (m, 3H), 4.64–4.55 (m, 1H), 4.36 (dd, J = 13.1, 3.2 Hz, 1H), 4.04–3.95 (m, 1H), 3.76–3.61 (m, 2H), 2.24–2.16 (m, 1H), 2.13–2.04 (m, 1H), 1.97–1.88 (m, 1H), 1.84–1.73 (m, 2H). ¹³C NMR (125 MHz, CDCl₃): δ 165.0, 157.7, 157.2, 152.7, 150.7, 150.2, 135.6, 134.2, 132.6, 129.6, 128.9, 125.2, 125.0, 123.1, 121.3, 116.0, 115.4, 71.4, 53.4, 50.3, 30.1, 22.9. HRMS (ESI): calcd for $C_{24}H_{23}N_4O$ [M + H]⁺, 383.1866; found, 383.1883.

4-(2-Benzylpiperidin-1-yl)-2-(pyridin-3-yl)quinazolin-4-amine (9d). Yellow solid (yield: 42%). ¹H NMR (500 MHz, CDCl₃): δ 9.72 (s, 1H), 8.76 (d, J = 7.9 Hz, 1H), 8.69 (d, J = 4.6 Hz, 1H), 7.90 (d, J = 8.4 Hz, 1H), 7.73 (d, J = 8.3 Hz, 1H), 7.70 (d, J = 7.0 Hz, 1H), 7.40 (dd, J = 7.8, 4.9 Hz, 1H), 7.36 (d, J = 7.1 Hz, 1H), 7.22–7.15 (m, 4H), 7.12 (d, J = 6.4 Hz, 1H), 5.00–5.06 (m, 1H), 4.30 (d, J = 13.2 Hz, 1H), 3.68–3.55 (m, 1H), 3.26 (dd, J = 13.5, 6.6 Hz, 1H), 3.09 (dd, J = 13.5, 8.8 Hz, 1H), 2.01–1.67 (m, 6H). ¹³C NMR (125 MHz, CDCl₃): δ 165.2, 157.7, 152.9, 150.7, 150.4, 139.0, 135.7, 134.5, 132.4, 129.2, 128.8, 128.5, 126.4, 125.1, 124.7, 123.2, 115.6, 58.0, 45.4, 35.8, 27.3, 25.9, 19.5. HRMS (ESI): calcd for $C_{25}H_{25}N_4$ [M + H]⁺, 381.2074; found, 381.2084.

4-(3-Benzylpiperidin-1-yl)-2-(pyridin-3-yl)quinazolin-4-amine (9e). Off-white solid (yield: 46%). ¹H NMR (500 MHz, CDCl₃): δ 9.70 (s, 1H), 8.68 (d, J = 7.6 Hz, 2H), 7.92 (d, J = 8.2 Hz, 1H), 7.71–7.59 (m, 2H), 7.44–7.36 (m, 1H), 7.36–7.29 (m, 2H), 7.27–7.23 (m, 2H), 7.21 (d, J = 7.1 Hz, 2H), 4.43 (dd, J = 30.6, 13.0 Hz, 2H), 3.30–3.14 (m, 1H), 2.91 (dd, J = 13.0, 10.7 Hz, 1H), 2.69 (dd, J = 13.5, 6.5 Hz, 1H), 2.60 (dd, J = 13.5, 8.1 Hz, 1H), 2.24–2.08 (m, 1H), 2.06–1.95 (m, 1H), 1.95–1.84 (m, 1H), 1.84–1.67 (m, 1H), 1.48–1.30 (m, 1H). ¹³C NMR (125 MHz, CDCl₃): δ 164.6, 157.6, 152.7, 150.7, 150.3, 139.8, 135.7, 132.5, 129.1, 128.8, 128.6, 126.3, 125.1, 125.0, 123.3, 115.5, 55.6, 50.6, 40.7, 38.6, 31.7, 25.7. HRMS (ESI): calcd for $C_{25}H_{25}N_4$ [M + H]⁺, 381.2074; found, 381.2089.

4-(3-Phenylpiperidin-1-yl)-2-(pyridin-3-yl)quinazolin-4-amine (9f). Yellow solid (yield: 34%). ¹H NMR (500 MHz, CDCl₃): δ 9.68 (s, 1H), 8.73 (d, J = 7.9 Hz, 1H), 8.61 (d, J = 3.9 Hz, 1H), 7.87 (dd, J = 17.0, 8.3 Hz, 2H), 7.66 (s, 1H), 7.38–7.27 (m, 5H), 7.25–7.18 (m, 2H), 4.58–4.45 (m, 2H), 3.24–3.13 (m, 2H), 3.08–2.98 (m, 1H), 2.12 (d, J = 12.3 Hz, 1H), 1.96–1.73 (m, 3H). ¹³C NMR (125 MHz, CDCl₃): δ 165.0, 157.7, 152.8, 150.8, 150.3, 143.5, 135.7, 134.3, 132.6, 129.0, 128.8, 127.2, 126.9, 125.3, 125.2, 123.2, 115.8, 56.6, 50.8, 42.8, 32.2, 25.9. HRMS (ESI): calcd for $C_{24}H_{23}N_4$ [M + H]⁺, 367.1917; found, 367.1930.

4-(3,4-Dihydroisoquinolin-2(1H)-yl)-2-(pyridin-3-yl)quinazolin-4-amine (9g). Yellow solid (yield: 44%). ¹H NMR (400 MHz, CDCl₃): δ 9.79 (s, 1H), 8.83 (d, J = 7.9 Hz, 1H), 8.71 (s, 1H), 7.99 (dd, J = 14.1, 8.4 Hz, 2H), 7.81–7.69 (m, 1H), 7.53–7.37 (m, 2H), 7.23 (s, 4H), 5.07 (s, 2H), 4.15 (t, J = 5.7 Hz, 2H), 3.22 (t, J = 5.6 Hz, 2H). ¹³C NMR (100 MHz, CDCl₃): δ 164.2, 157.6, 152.8, 150.8, 150.4, 135.8, 134.8, 133.9, 132.6, 129.0, 128.9, 126.9, 126.6, 126.5, 125.2, 125.0, 123.3, 115.6, 51.4, 48.2, 29.0. HRMS (ESI): calcd for $C_{22}H_{19}N_4$ [M + H]⁺, 339.1604; found, 339.1613.

2-(2-(Pyridin-3-yl)quinazolin-4-yl)-2,3,4,5-tetrahydro-1H-pyridolo[4,3-b]indole (9h). Light-brown solid (yield: 37%). ¹H NMR (500 MHz, CDCl₃): δ 9.78 (s, 1H), 8.81 (d, J = 7.9 Hz, 1H), 8.69 (d, J = 3.7 Hz, 1H), 8.21 (s, 1H), 8.04 (d, J = 8.2 Hz, 1H), 7.94 (d, J = 8.3 Hz, 1H), 7.74 (t, J = 7.6 Hz, 1H), 7.48 (t, J = 7.8 Hz, 2H), 7.41 (dd, J = 7.8, 4.8 Hz, 1H), 7.30 (d, J = 8.0 Hz, 1H), 7.17–7.11 (m, 1H), 7.11–7.05 (m, 1H), 5.14 (s, 2H), 4.27 (t, J = 5.5 Hz, 2H), 3.29–3.17 (m, 2H). ¹³C NMR (125 MHz, CDCl₃): δ 164.6, 157.5, 152.8, 150.7, 150.2, 135.9, 135.7, 134.2, 132.6, 132.2, 128.9, 125.5, 125.2, 125.0, 123.2, 121.7, 119.7, 117.4, 115.6, 110.8, 107.8, 47.7, 47.0, 23.4. HRMS (ESI): calcd for $C_{24}H_{20}N_5$ [M + H]⁺, 378.1713; found, 378.1727.

2-(2-(Pyridin-3-yl)quinazolin-4-yl)-2,3,4,9-tetrahydro-1H-pyridolo[3,4-b]indole (9i). Yellow solid (yield: 62%). ¹H NMR (500 MHz, CDCl₃): δ 9.75 (s, 1H), 8.79 (d, J = 7.9 Hz, 1H), 8.68 (d, J = 3.7 Hz, 1H), 8.38 (s, 1H), 8.02–7.91 (m, 2H), 7.73 (t, J = 7.6 Hz, 1H), 7.54 (d, J = 7.6 Hz, 1H), 7.48–7.42 (m, 1H), 7.39 (dd, J = 7.8, 4.8 Hz, 1H), 7.35 (d, J = 7.9 Hz, 1H), 7.21–7.10 (m, 2H), 4.99 (s, 2H), 4.14 (t, J = 5.3 Hz, 2H), 3.18 (d, J = 4.7 Hz, 2H). ¹³C NMR (125 MHz, CDCl₃): δ 164.5, 157.4, 152.6, 150.7, 150.1, 136.3, 135.7, 134.1, 132.7, 130.9, 129.0, 127.0, 125.4, 124.6, 123.2, 121.8, 119.7, 118.0, 115.5, 111.0, 108.9, 49.8, 46.8, 22.0. HRMS (ESI): calcd for $C_{24}H_{20}N_5$ [M + H]⁺, 378.1713; found, 378.1728.

4-(2-(Pyridin-3-yl)quinazolin-4-yl)-1,4-oxazepane (9j). White solid (yield: 58%). ¹H NMR (500 MHz, CDCl₃): δ 9.71 (d, J = 1.0 Hz, 1H), 8.81–8.57 (m, 2H), 7.93 (dd, J = 12.0, 8.4 Hz, 2H), 7.74–7.66 (m, 1H), 7.43–7.34 (m, 2H), 4.18–4.10 (m, 4H), 4.03–3.99 (m, 2H), 3.85–3.80 (m, 2H), 2.21 (p, J = 5.7 Hz, 2H). ¹³C NMR (125 MHz, CDCl₃): δ 163.3, 157.2, 153.1, 150.6, 150.1, 135.5, 132.3, 128.9, 125.2, 124.5, 114.9, 70.2, 70.1, 53.7, 50.3, 30.7. HRMS (ESI): calcd for $C_{18}H_{19}N_4O$ [M + H]⁺, 307.1553; found, 307.1557.

4-(2-(Pyridin-3-yl)quinazolin-4-yl)-2,3,4,5-tetrahydrobenzof[1,4]oxazepine (9k). Yellow solid (yield: 55%). ¹H NMR (500 MHz, CDCl₃): δ 9.62 (s, 1H), 8.72–8.59 (m, 2H), 7.94 (t, J = 8.1 Hz, 2H), 7.77–7.68 (m, 1H), 7.45–7.39 (m, 1H), 7.39–7.31 (m, 2H), 7.22 (d, J = 7.5 Hz, 1H), 7.10 (t, J = 7.2 Hz, 1H), 7.02 (d, J = 7.9 Hz, 1H), 4.97 (s, 2H), 4.48–4.39 (m, 2H), 4.35–4.26 (m, 2H). ¹³C NMR (125 MHz, CDCl₃): δ 164.4, 159.3, 157.4, 152.8, 150.7, 150.2, 135.6, 132.6, 129.9, 129.0, 128.9, 128.7, 125.2, 125.1, 123.1, 120.5, 115.2,

70.9, 54.5, 54.0. HRMS (ESI): calcd for $C_{22}H_{19}N_4O$ $[M + H]^+$, 355.1553; found, 355.1565.

N-Methyl-N-(naphthalen-2-ylmethyl)-2-(pyridin-3-yl)quinazolin-4-amine (9l). Off-white solid (yield: 52%). 1H NMR (500 MHz, $CDCl_3$): δ 9.77 (s, 1H), 8.83 (d, $J = 7.8$ Hz, 1H), 8.69 (d, $J = 3.5$ Hz, 1H), 7.99 (d, $J = 8.6$ Hz, 2H), 7.95–7.78 (m, 4H), 7.78–7.67 (m, 1H), 7.58–7.44 (m, 3H), 7.41 (dd, $J = 7.7, 4.9$ Hz, 1H), 7.37–7.28 (m, 1H), 5.23 (s, 2H), 3.45 (s, 3H). ^{13}C NMR (125 MHz, $CDCl_3$): δ 164.0, 157.5, 152.9, 150.8, 150.3, 135.8, 134.9, 134.3, 133.6, 133.0, 132.6, 129.0, 128.9, 127.9, 126.6, 126.1, 125.9, 125.3, 125.2, 125.1, 123.3, 115.1, 57.4, 39.7. HRMS (ESI): calcd for $C_{25}H_{21}N_4$ $[M + H]^+$, 377.1761; found, 377.1775.

N-(Benzo[c][1,2,5]thiadiazol-5-ylmethyl)-N-methyl-2-(pyridin-3-yl)quinazolin-4-amine (9m). Pale yellow solid (yield: 65%). 1H NMR (500 MHz, $CDCl_3$): δ 9.70 (d, $J = 1.6$ Hz, 1H), 8.77 (dt, $J = 7.9, 1.8$ Hz, 1H), 8.67 (dd, $J = 4.8, 1.6$ Hz, 1H), 8.07–8.02 (m, 2H), 8.00 (t, $J = 8.1$ Hz, 2H), 7.79–7.70 (m, 1H), 7.64 (dd, $J = 9.1, 1.4$ Hz, 1H), 7.43–7.32 (m, 2H), 5.24 (s, 2H), 3.49 (s, 3H). ^{13}C NMR (125 MHz, $CDCl_3$): δ 163.9, 157.5, 155.2, 154.6, 153.1, 150.9, 150.3, 139.7, 135.7, 134.1, 132.8, 129.5, 129.2, 125.2, 125.0, 123.3, 122.2, 119.2, 115.1, 56.8, 40.3. HRMS (ESI): calcd for $C_{21}H_{17}N_6S$ $[M + H]^+$, 385.1230; found, 385.1245.

N-Methyl-N-((2-methylisoindolin-5-yl)methyl)-2-(pyridin-3-yl)quinazolin-4-amine (9n). Light-brown solid (yield: 61%). 1H NMR (400 MHz, $CDCl_3$): δ 9.73 (d, $J = 1.5$ Hz, 1H), 8.79 (dt, $J = 8.0, 1.9$ Hz, 1H), 8.68 (dd, $J = 4.8, 1.7$ Hz, 1H), 7.99–7.91 (m, 2H), 7.77–7.68 (m, 1H), 7.39 (dd, $J = 7.9, 4.8$ Hz, 1H), 7.36–7.29 (m, 1H), 7.28–7.21 (m, 4H), 5.05 (s, 2H), 3.97 (d, $J = 6.7$ Hz, 4H), 3.38 (s, 3H), 2.64 (s, 3H). ^{13}C NMR (100 MHz, $CDCl_3$): δ 163.9, 157.6, 153.0, 150.8, 136.2, 135.7, 134.3, 132.5, 128.9, 126.1, 125.2, 125.0, 123.2, 122.8, 121.1, 115.1, 60.9, 60.8, 57.1, 42.4, 39.6. HRMS (ESI): calcd for $C_{24}H_{24}N_5$ $[M + H]^+$, 382.2026; found, 382.2040.

N-(Benzo[d][1,3]dioxol-5-ylmethyl)-N-methyl-2-(pyridin-3-yl)quinazolin-4-amine (9o). Yellow solid (yield: 43%). 1H NMR (400 MHz, $CDCl_3$): δ 9.74 (s, 1H), 8.80 (d, $J = 8.0$ Hz, 1H), 8.68 (d, $J = 3.3$ Hz, 1H), 7.97 (d, $J = 8.8$ Hz, 2H), 7.76–7.66 (m, 1H), 7.40 (dd, $J = 7.8, 4.8$ Hz, 1H), 7.37–7.32 (m, 1H), 6.89 (d, $J = 9.4$ Hz, 2H), 6.83 (d, $J = 7.8$ Hz, 1H), 5.97 (s, 2H), 4.98 (s, 2H), 3.37 (s, 3H). ^{13}C NMR (100 MHz, $CDCl_3$): δ 163.8, 157.5, 152.9, 150.8, 150.3, 148.4, 147.2, 135.8, 132.5, 131.2, 128.9, 125.2, 125.0, 123.3, 120.7, 115.1, 108.6, 107.8, 101.2, 56.7, 39.6. HRMS (ESI): calcd for $C_{22}H_{19}N_4O_2$ $[M + H]^+$, 371.1503; found, 371.1518.

N-((2,3-Dihydrobenzo[b][1,4]dioxin-6-yl)methyl)-N-methyl-2-(pyridin-3-yl)quinazolin-4-amine (9p). Pale-yellow solid (yield: 36%). 1H NMR (500 MHz, $CDCl_3$): δ 9.73 (s, 1H), 8.79 (d, $J = 7.9$ Hz, 1H), 8.67 (d, $J = 4.6$ Hz, 1H), 7.95 (t, $J = 8.0$ Hz, 2H), 7.74–7.66 (m, 1H), 7.39 (dd, $J = 7.7, 4.9$ Hz, 1H), 7.36–7.30 (m, 1H), 6.94 (s, 1H), 6.89 (s, 2H), 4.95 (s, 2H), 4.27 (s, 4H), 3.37 (s, 3H). ^{13}C NMR (125 MHz, $CDCl_3$): δ 163.8, 157.5, 153.0, 150.8, 150.3, 144.0, 143.1, 135.7, 134.3, 132.5, 130.6, 128.9, 125.2, 124.9, 123.2, 120.3, 117.7, 116.1, 115.1, 64.5, 64.4, 56.5, 39.5. HRMS (ESI): calcd for $C_{23}H_{21}N_4O_2$ $[M + H]^+$, 385.1659; found, 385.1683.

(S)-N-((2,3-Dihydrobenzo[b][1,4]dioxin-2-yl)methyl)-N-methyl-2-(pyridin-3-yl)quinazolin-4-amine (9q). Pale-yellow solid (yield: 85%). 1H NMR (500 MHz, $CDCl_3$): δ 9.65 (s, 1H), 8.72 (d, $J = 7.9$ Hz, 1H), 8.69–8.64 (m, 1H), 8.13 (d, $J = 8.4$ Hz, 1H), 7.93 (d, $J = 8.4$ Hz, 1H), 7.76–7.68 (m, 1H), 7.43–7.34 (m, 2H), 6.90–6.78 (m, 4H), 4.84–4.76 (m, 1H), 4.40–4.27 (m, 2H), 4.17–4.08 (m, 2H), 3.66 (s, 3H). ^{13}C NMR (125 MHz, $CDCl_3$): δ 163.0, 157.1, 153.1, 150.8, 150.0, 143.1, 142.6, 135.5, 134.1, 132.5, 128.9, 125.5, 124.7, 123.2, 121.8, 121.5, 117.4, 117.2, 115.0, 71.8, 66.0, 53.0, 43.1. HRMS (ESI): calcd for $C_{23}H_{21}N_4O_2$ $[M + H]^+$, 385.1659; found, 385.1657.

(R)-N-((2,3-Dihydrobenzo[b][1,4]dioxin-2-yl)methyl)-N-methyl-2-(pyridin-3-yl)quinazolin-4-amine (9r). Pale-yellow solid (yield: 89%). 1H NMR (500 MHz, $CDCl_3$): δ 9.65 (s, 1H), 8.72 (d, $J = 7.9$ Hz, 1H), 8.69–8.64 (m, 1H), 8.13 (d, $J = 8.4$ Hz, 1H), 7.93 (d, $J = 8.4$ Hz, 1H), 7.76–7.68 (m, 1H), 7.43–7.34 (m, 2H), 6.90–6.78 (m, 4H), 4.84–4.76 (m, 1H), 4.40–4.27 (m, 2H), 4.17–4.08 (m, 2H), 3.66 (s, 3H). ^{13}C NMR (125 MHz, $CDCl_3$): δ 163.0, 157.1,

153.1, 150.8, 150.0, 143.1, 142.6, 135.5, 134.1, 132.5, 128.9, 125.5, 124.7, 123.2, 121.8, 121.5, 117.4, 117.2, 115.0, 71.8, 66.0, 53.0, 43.1. HRMS (ESI): calcd for $C_{23}H_{21}N_4O_2$ $[M + H]^+$, 385.1659; found, 385.1653.

N-Methyl-2-(pyridin-3-yl)-N-(quinoxalin-2-ylmethyl)quinazolin-4-amine (9s). Yellow solid (yield: 47%). 1H NMR (500 MHz, $CDCl_3$): δ 9.65 (s, 1H), 9.02 (s, 1H), 8.70 (d, $J = 7.7$ Hz, 1H), 8.65 (d, $J = 2.4$ Hz, 1H), 8.14 (d, $J = 8.4$ Hz, 1H), 8.10 (d, $J = 8.1$ Hz, 2H), 7.99 (d, $J = 8.3$ Hz, 1H), 7.83–7.72 (m, 3H), 7.42 (t, $J = 7.6$ Hz, 1H), 7.35 (dd, $J = 7.2, 5.0$ Hz, 1H), 5.41 (s, 2H), 3.63 (s, 3H). ^{13}C NMR (125 MHz, $CDCl_3$): δ 163.5, 157.4, 153.2, 153.1, 150.8, 150.1, 144.7, 142.1, 135.7, 134.0, 132.8, 130.4, 129.9, 129.4, 129.2, 129.1, 125.3, 125.2, 123.3, 115.0, 57.0, 41.4. HRMS (ESI): calcd for $C_{23}H_{19}N_6$ $[M + H]^+$, 379.1666; found, 379.1682.

N-(Benzo[d]thiazol-2-ylmethyl)-N-methyl-2-(pyridin-3-yl)quinazolin-4-amine (9t). Yellow solid (yield: 26%). 1H NMR (400 MHz, $CDCl_3$): δ 9.80 (s, 1H), 8.84 (d, $J = 8.0$ Hz, 1H), 8.69 (d, $J = 3.6$ Hz, 1H), 8.13 (d, $J = 8.3$ Hz, 1H), 8.02 (dd, $J = 16.6, 8.2$ Hz, 2H), 7.81 (d, $J = 7.9$ Hz, 1H), 7.78 (d, $J = 8.1$ Hz, 1H), 7.48 (d, $J = 7.3$ Hz, 1H), 7.46–7.34 (m, 3H), 5.44 (s, 2H), 3.58 (s, 3H). ^{13}C NMR (100 MHz, $CDCl_3$): δ 168.5, 163.2, 157.2, 153.1, 152.8, 150.9, 150.4, 135.9, 135.8, 133.8, 132.9, 129.1, 126.2, 125.4, 125.3, 125.3, 123.3, 123.0, 121.9, 115.0, 54.8, 40.8. HRMS (ESI): calcd for $C_{22}H_{18}N_5S$ $[M + H]^+$, 384.1277; found, 384.1293.

N-((1H-Benzo[d]imidazol-2-yl)methyl)-N-methyl-2-(pyridin-3-yl)quinazolin-4-amine (9u). Yellow solid (yield: 41%). 1H NMR (400 MHz, $CDCl_3$): δ 9.61 (s, 1H), 8.66 (dt, $J = 8.0, 1.9$ Hz, 1H), 8.61–8.48 (m, 1H), 8.03 (d, $J = 8.3$ Hz, 1H), 7.92 (d, $J = 8.3$ Hz, 1H), 7.79–7.68 (m, 1H), 7.57 (br s, 2H), 7.46–7.33 (m, 1H), 7.26–7.20 (m, 3H), 5.27 (s, 2H), 3.47 (s, 3H). ^{13}C NMR (100 MHz, $CDCl_3$): δ 163.4, 156.9, 152.9, 151.1, 150.7, 149.5, 135.5, 133.7, 133.2, 128.9, 125.6, 125.5, 123.4, 122.8, 114.9, 50.5, 40.7. HRMS (ESI): calcd for $C_{22}H_{19}N_6$ $[M + H]^+$, 367.1666; found, 367.1683.

N-(Benzo[d]oxazol-2-ylmethyl)-N-methyl-2-(pyridin-3-yl)quinazolin-4-amine (9v). Off-white solid (yield: 35%). 1H NMR (500 MHz, $CDCl_3$): δ 9.66 (d, $J = 1.5$ Hz, 1H), 8.73 (dt, $J = 7.9, 1.8$ Hz, 1H), 8.65 (dd, $J = 4.8, 1.6$ Hz, 1H), 8.21 (d, $J = 7.9$ Hz, 1H), 7.99 (d, $J = 8.3$ Hz, 1H), 7.82–7.75 (m, 1H), 7.75–7.70 (m, 1H), 7.59–7.51 (m, 1H), 7.50–7.44 (m, 1H), 7.38–7.30 (m, 3H), 5.25 (s, 2H), 3.71 (s, 3H). ^{13}C NMR (125 MHz, $CDCl_3$): δ 163.5, 163.1, 157.2, 153.0, 150.9, 150.7, 150.1, 141.1, 135.9, 134.0, 132.9, 129.1, 125.4, 125.3, 125.3, 124.7, 123.3, 120.2, 115.1, 110.8, 50.4, 41.7. HRMS (ESI): calcd for $C_{22}H_{18}N_5O$ $[M + H]^+$, 368.1506; found, 368.1518.

N-Methyl-N-(2-phenoxyethyl)-2-(pyridin-2-yl)quinazolin-4-amine (11a). Pale-yellow solid (yield: 73%). 1H NMR (500 MHz, $CDCl_3$): δ 8.85 (d, $J = 4.7$ Hz, 1H), 8.48 (d, $J = 7.9$ Hz, 1H), 8.16 (d, $J = 8.4$ Hz, 1H), 8.13 (d, $J = 8.5$ Hz, 1H), 7.81 (td, $J = 7.7, 1.8$ Hz, 1H), 7.71 (ddd, $J = 8.3, 7.0, 1.3$ Hz, 1H), 7.40 (ddd, $J = 8.3, 7.0, 1.2$ Hz, 1H), 7.37–7.32 (m, 1H), 7.27–7.24 (m, 2H), 6.97–6.87 (m, 3H), 4.44 (t, $J = 5.6$ Hz, 2H), 4.28 (t, $J = 5.6$ Hz, 2H), 3.61 (s, 3H). ^{13}C NMR (125 MHz, $CDCl_3$): δ 163.5, 158.5, 157.9, 156.0, 153.2, 150.0, 136.6, 132.2, 129.8, 129.5, 125.2, 124.9, 124.2, 123.6, 121.1, 115.3, 114.5, 65.8, 52.4, 41.7. HRMS (ESI): calcd for $C_{22}H_{21}N_4O$ $[M + H]^+$, 357.1710; found, 357.1724.

N-Methyl-N-(2-phenoxyethyl)-2-(pyridin-4-yl)quinazolin-4-amine (11b). White solid (yield: 56%). 1H NMR (500 MHz): δ 9.69 (s, 1H), 8.75 (dd, $J = 7.9, 1.7$ Hz, 1H), 8.67 (d, $J = 4.0$ Hz, 1H), 8.13 (d, $J = 8.5$ Hz, 1H), 7.92 (d, $J = 8.4$ Hz, 1H), 7.73–7.68 (m, 1H), 7.41–7.35 (m, 2H), 7.26 (d, $J = 8.4$ Hz, 2H), 6.95–6.87 (m, 3H), 4.45 (t, $J = 5.4$ Hz, 2H), 4.28 (t, $J = 5.4$ Hz, 2H), 3.68 (s, 3H), 3.63 (s, 3H). ^{13}C NMR (125 MHz, $CDCl_3$): δ 163.2, 158.5, 157.0, 152.9, 150.2, 146.2, 132.4, 129.6, 129.0, 125.5, 125.0, 122.2, 121.1, 115.3, 114.5, 65.8, 52.5, 41.7. HRMS (ESI): calcd for $C_{22}H_{21}N_4O$ $[M + H]^+$, 357.1710; found, 357.1721.

N-Methyl-N-(2-phenoxyethyl)-2-(pyrimidin-5-yl)quinazolin-4-amine (11c). White solid (yield: 61%). 1H NMR (500 MHz, $CDCl_3$): δ 9.73 (s, 2H), 9.27 (s, 1H), 8.15 (d, $J = 8.4$ Hz, 1H), 7.93 (d, $J = 8.3$ Hz, 1H), 7.76–7.70 (m, 1H), 7.45–7.40 (m, 1H), 7.29–7.24 (m, 2H), 6.93 (t, $J = 7.4$ Hz, 1H), 6.89 (d, $J = 7.9$ Hz, 2H), 4.44 (t, $J = 5.3$ Hz, 2H), 4.28 (t, $J = 5.3$ Hz, 2H), 3.64 (s, 3H). ^{13}C NMR (125 MHz,

CDCl₃): δ 162.0, 158.2, 157.4, 155.7, 154.0, 151.8, 131.5, 130.8, 128.5, 127.8, 124.6, 124.0, 120.1, 114.2, 113.4, 64.8, 51.5, 40.9. HRMS (ESI): calcd for C₂₁H₂₀N₅O [M + H]⁺, 358.1662; found, 358.1673.

N-Methyl-N-(2-phenoxyethyl)-2-phenylquinazolin-4-amine (11d). White solid (yield: 82%). ¹H NMR (500 MHz, CDCl₃): δ 8.54–8.47 (m, 2H), 8.11 (d, *J* = 8.4 Hz, 1H), 7.94 (d, *J* = 8.2 Hz, 1H), 7.69 (ddd, *J* = 8.3, 6.9, 1.3 Hz, 1H), 7.48–7.43 (m, 3H), 7.36 (ddd, *J* = 8.3, 6.9, 1.2 Hz, 1H), 7.28–7.24 (m, 2H), 6.97–6.89 (m, 3H), 4.45 (t, *J* = 5.6 Hz, 2H), 4.27 (t, *J* = 5.6 Hz, 2H), 3.60 (s, 3H). ¹³C NMR (125 MHz, CDCl₃): δ 163.2, 159.0, 158.6, 132.1, 130.0, 129.5, 128.4, 128.3, 125.4, 124.2, 121.0, 114.5, 65.9, 52.4, 41.8. HRMS (ESI): calcd for C₂₁H₂₀N₆ [M + H]⁺, 356.1744; found, 356.1771.

N-Methyl-N-(2-phenoxyethyl)-2-(thiophen-3-yl)quinazolin-4-amine (11e). Pale-yellow solid (yield: 71%). ¹H NMR (500 MHz, CDCl₃): δ 8.26 (s, 1H), 8.08 (d, *J* = 8.4 Hz, 1H), 7.94 (dd, *J* = 5.0, 0.9 Hz, 1H), 7.88 (d, *J* = 7.5 Hz, 1H), 7.69–7.63 (m, 1H), 7.37–7.30 (m, 2H), 7.26 (dd, *J* = 8.6, 7.5 Hz, 2H), 6.96–6.90 (m, 3H), 4.43 (t, *J* = 5.6 Hz, 2H), 4.23 (t, *J* = 5.6 Hz, 2H), 3.58 (s, 3H). ¹³C NMR (125 MHz, CDCl₃): δ 163.2, 158.6, 156.4, 153.1, 142.8, 132.1, 129.5, 128.5, 127.8, 127.2, 125.4, 124.0, 121.0, 114.8, 114.6, 65.9, 52.4, 41.7. HRMS (ESI): calcd for C₂₁H₂₀N₃OS [M + H]⁺, 362.1322; found, 362.1336.

N-Methyl-N-(2-phenoxyethyl)-2-(thiophen-2-yl)quinazolin-4-amine (11f). Pale-yellow solid (yield: 45%). ¹H NMR (500 MHz, CDCl₃): δ 8.06 (d, *J* = 8.4 Hz, 1H), 8.00 (s, 1H), 7.86 (s, 1H), 7.66 (t, *J* = 7.4 Hz, 1H), 7.41 (d, *J* = 4.8 Hz, 1H), 7.36–7.29 (m, 1H), 7.28–7.24 (m, 2H), 7.14–7.11 (m, 1H), 6.95–6.89 (m, 3H), 4.46 (t, *J* = 5.5 Hz, 2H), 4.22 (t, *J* = 5.5 Hz, 2H), 3.60 (s, 3H). ¹³C NMR (125 MHz, CDCl₃): δ 162.8, 158.6, 155.9, 153.0, 145.0, 132.3, 129.5, 128.8, 128.3, 128.0, 125.5, 124.0, 121.0, 114.8, 114.5, 65.9, 52.6, 41.9. HRMS (ESI): calcd for C₂₁H₂₀N₃OS [M + H]⁺, 362.1322; found, 362.1336.

2-(Furan-2-yl)-N-methyl-N-(2-phenoxyethyl)quinazolin-4-amine (11g). Yellow oil (yield: 40%). ¹H NMR (500 MHz, CDCl₃): δ 8.06 (dd, *J* = 8.5, 0.9 Hz, 1H), 7.95 (dd, *J* = 8.4, 0.8 Hz, 1H), 7.67 (ddd, *J* = 8.3, 6.9, 1.3 Hz, 1H), 7.61 (dd, *J* = 1.6, 0.8 Hz, 1H), 7.34 (ddd, *J* = 8.3, 6.9, 1.3 Hz, 1H), 7.29–7.22 (m, 3H), 6.96–6.90 (m, 3H), 6.53 (dd, *J* = 3.3, 1.7 Hz, 1H), 4.42 (t, *J* = 5.6 Hz, 2H), 4.20 (t, *J* = 5.6 Hz, 2H), 3.56 (s, 3H). ¹³C NMR (125 MHz, CDCl₃): δ 163.2, 158.5, 153.2, 152.8, 152.5, 144.5, 132.3, 129.5, 128.7, 125.4, 124.2, 121.0, 115.0, 114.5, 112.7, 111.7, 65.7, 52.4, 41.7. HRMS (ESI): calcd for C₂₁H₂₀N₃O₂ [M + H]⁺, 346.1550; found, 346.1559.

2-(Furan-3-yl)-N-methyl-N-(2-phenoxyethyl)quinazolin-4-amine (11h). Yellow solid (yield: 63%). ¹H NMR (500 MHz, CDCl₃): δ 8.21 (s, 1H), 8.06 (d, *J* = 8.4 Hz, 1H), 7.85 (d, *J* = 8.3 Hz, 1H), 7.69–7.63 (m, 1H), 7.47 (t, *J* = 1.7 Hz, 1H), 7.35–7.29 (m, 1H), 7.29–7.24 (m, 2H), 7.11 (d, *J* = 1.5 Hz, 1H), 6.96–6.92 (m, 1H), 6.91 (d, *J* = 7.9 Hz, 2H), 4.41 (t, *J* = 5.6 Hz, 2H), 4.19 (t, *J* = 5.6 Hz, 2H), 3.55 (s, 3H). ¹³C NMR (125 MHz, CDCl₃): δ 163.1, 158.6, 155.7, 153.0, 144.5, 143.4, 132.1, 129.5, 128.3, 127.9, 125.4, 123.9, 121.0, 114.9, 114.5, 109.9, 65.8, 52.3, 41.6. HRMS (ESI): calcd for C₂₁H₂₀N₃O₂ [M + H]⁺, 346.1550; found, 346.1561.

Enzyme Activity Assay. 4-Methylumbelliferyl β -D-glucopyranoside (4MU- β -Glc) and buffer components were purchased from Sigma-Aldrich (St. Louis, MO). Residual injection solutions of the recombinant wild-type GCase enzyme velaglycerase alfa (Vpriv, Shire Human Genetic Therapies, Inc.) in clinics were collected for the activity assays. The GCase activity assay buffer was composed of 50 mM citric acid, 176 mM K₂HPO₄, and 0.01% Tween-20 at pH 5.9. A solution of 1 M sodium hydroxide and 1 M glycine was used as the stop solution.

The compounds in DMSO solution (0.5 μ L/well) were transferred to a black 96-well plate (the final titration was 48 nM to 100 μ M, a 12-point dilution series). The enzyme solution (33.5 μ L, 7.5 nM final concentration) was transferred to the wells. After 5 min of incubation at room temperature, the enzyme reaction was initiated by the addition of a blue substrate (4MU- β -Glc) (33 μ L/well). The final concentration of the blue substrate was 1.5 mM. The blue substrate

reaction was terminated by the addition of 33 μ L/well stop solution (1 M NaOH and 1 M glycine mixture, pH 10) after 30 min of incubation at 37 °C. The fluorescence was then measured in a Biotek Synergy H1 multimode plate reader with λ_{ex} = 365 nm and λ_{em} = 440 nm.

Cell Culture and Compound Treatment. The GBA N370S/84GG fibroblast cell line was obtained from Coriell, GM00372, cultured in DMEM medium (Life Tech) including 1% v/v L-glutamine 200 mM (Life Tech), 1% v/v pen strep (Life Tech), 10% FBS (Life Tech) at 37 °C, and 5% CO₂ and treated with different compounds at indicated concentrations. The same volume of DMSO (0.1% v/v) was used as a control. After a 3 day treatment for fibroblasts or a 10 day treatment for dopaminergic neurons, cells were washed with PBS twice followed by 1% Triton X-100 lysis buffer to lyse cells. Protein concentrations were measured with a BCA kit (Thermo), and the GCase activity was determined at pH 5.5.

Measurement of Lysosomal GCase Activity. Fibroblasts were plated into a 96-well plate and cultured and treated with compounds as described above. After 3 days of treatment, the medium was replaced with media containing 5-(pentafluorobenzoylamino)-fluorescein di- β -D-glucopyranoside (PFB-FDGLu) or media containing PFB-FDGLu with 400 μ M bafilomycin. Cells were incubated for 1 h to allow for loading of the substrate into the lysosome. After loading, substrate hydrolysis was monitored by measuring fluorescence unquenching every 20 min at 485 nm excitation and 525 nm emission.

Human iPSC Culture and Neural Differentiation. Human iPSC lines were generated from skin fibroblasts through retroviral expression or using Sendai virus based delivery of key reprogramming vectors including four Yamanaka factors (Oct, Sox2, Klf4, and c-Myc).²³ Heterozygous N370S GBA1 mutant fibroblasts were reprogrammed into iPSC through Northwestern University Stem Cell Core Facility and characterized in this study (see Supporting Information figure).

The iPSC line from one separate healthy control subject was previously described and characterized.²⁴ Healthy control and GBA1 mutant iPSC lines were characterized for expression of pluripotent markers by immunocytochemistry (NANOG, OCT4, SSEA4, and TRA1-81). Karyotype analysis was performed by Cell Line Genetics using standard protocols for high-resolution G-banding. iPSC were cultured in mTeSR media (Stem Cell Technologies) and passaged every 5–7 days on matrigel (Corning) coated plates. All lines were routinely tested for mycoplasma contamination.

Differentiation of iPSCs into midbrain dopaminergic neurons was done according to published protocols,²⁵ passaged and maintained as described previously.²⁶ At d25 to d30, neural blocks were passed by accutase treatment onto PDL/laminin-coated culture dishes. Neutralization growth factors were withdrawn at d40, and neurons were maintained in Neurobasal media (Life Technologies) containing Neurocult SM1 (Stemcell technologies). Immunocytochemistry demonstrated the neuralization efficiency in neurons derived from iPSC lines using neural (β -III-tubulin) and midbrain (TH, FOXA2, LMX1a) specific markers.

Sequencing Analysis. DNA samples were extracted from cell pellets using Mini prep kits (Qiagen). Eluted gDNA was used as a template for PCR amplification using Phusion Master Mix (NEB). The PCR product was purified using the PCR Purification Kit (Qiagen) and sent for sequencing through Northwestern University Seq Core or University of Chicago Seq Core.

Deglycosylation of Proteins/Molecular Shift Assay.²² To study the subcellular localization and transport of the various GCase mutants (ER and post-ER localization), EndoH and PNGaseF digestions were performed. For both reactions, 20 μ g of protein was used, and the experimental procedure was performed according to the manufacturer's handbook (New England Biolabs). A positive digestion resulted in a shift in molecular size after the protein was subjected to SDS/PAGE. Anti-hGCase (From Johannes Aerts, Leiden University, Leiden, The Netherlands) was used to detect the different forms of GCase.

Western Blots. Proteins were denatured in 20% SDS sample buffer at 100 °C for 10 min; 10% Tris-glycine (Life Tech) was used for gels; a Trans-Blot Turbo PVDF kit (Bio-Rad) was used for membrane transfer. GCase antibody (Sigma-Aldrich) and GAPDH primary antibodies (EMD Millipore) were incubated with the membranes overnight, and then the incubated membranes were treated with the secondary antibody (IRDye 680RD goat anti-rabbit IgG (H + L) or IRDye 800CW Goat anti-mouse IgG (H + L), LI-COR) for 30 min. An Odyssey CLx Imaging System (LI-COR) was used to scan the membranes and analyze the imaging.

■ ASSOCIATED CONTENT

Supporting Information

The Supporting Information is available free of charge on the ACS Publications website at DOI: 10.1021/acs.jmedchem.8b01294.

Characterization of iPSC lines and differentiated dopaminergic neurons. ¹H and ¹³C NMR spectra of **6a**, **8a**, **9l**, **9o**, **9q**, **9s**, **11a**, and **11b** (PDF)
Molecular formula strings (CSV)

■ AUTHOR INFORMATION

Corresponding Authors

*E-mail: dkrainc@nm.org. Phone: 312-503-3936. Fax: 312-503-3950 (D.K.).

*E-mail: Agman@chem.northwestern.edu. Phone: 847-491-5653. Fax: 847-491-7713 (R.B.S.).

ORCID

Dimitri Krainc: 0000-0002-4716-1886

Richard B. Silverman: 0000-0001-9034-1084

Notes

The authors declare no competing financial interest.

■ ACKNOWLEDGMENTS

This work was supported by NIH R01NS076054, R01NS096240, WildKat and Buckeye Research LLC (to D.K.) and The Michael J. Fox Foundation for Parkinson's Research (to J.Z.). This work made use of the IMSERC at Northwestern University, which has received support from the Soft and Hybrid Nanotechnology Experimental (SHyNE) Resource (NSF NNCI-1542205); the State of Illinois and International Institute for Nanotechnology (IIN). We would like to thank H. Goudarzi and S. Shafaie in IMSERC at Northwestern University for their assistance with HRMS experiments. We thank the Northwestern Stem Cell Core Facility for the generation of iPSC lines from the GBA1 mutation carrier.

■ ABBREVIATIONS

GD, Gaucher's disease; GCase, β -glucocerebrosidase; ER, endoplasmic reticulum; PC, pharmacological chaperone; IFG, isofagomine; PD, Parkinson's disease; DLB, dementia with Lewy bodies; SAR, structure–activity relationship

■ REFERENCES

- (1) Aharon-Peretz, J.; Rosenbaum, H.; Gershoni-Baruch, R. Mutations in the glucocerebrosidase gene and Parkinson's disease in Ashkenazi Jews. *N. Engl. J. Med.* **2004**, *351*, 1972–1977.
- (2) Sidransky, E.; Nalls, M. A.; Aasly, J. O.; Aharon-Peretz, J.; Annesi, G.; Barbosa, E. R.; Bar-Shira, A.; Berg, D.; Bras, J.; Brice, A.; Chen, C.-M.; Clark, L. N.; Condroyer, C.; De Marco, E. V.; Dürr, A.; Eblan, M. J.; Fahn, S.; Farrer, M. J.; Fung, H.-C.; Gan-Or, Z.; Gasser, T.; Gershoni-Baruch, R.; Giladi, N.; Griffith, A.; Gurevich, T.;

Januario, C.; Kropp, P.; Lang, A. E.; Lee-Chen, G.-J.; Lesage, S.; Marder, K.; Mata, I. F.; Mirelman, A.; Mitsui, J.; Mizuta, I.; Nicoletti, G.; Oliveira, C.; Ottman, R.; Orr-Urtreger, A.; Pereira, L. V.; Quattrone, A.; Rogaeva, E.; Rolfs, A.; Rosenbaum, H.; Rozenberg, R.; Samii, A.; Samadpour, T.; Schulte, C.; Sharma, M.; Singleton, A.; Spitz, M.; Tan, E.-K.; Tayebi, N.; Toda, T.; Troiano, A. R.; Tsuji, S.; Wittstock, M.; Wolfsberg, T. G.; Wu, Y.-R.; Zabetian, C. P.; Zhao, Y.; Ziegler, S. G. Multicenter analysis of glucocerebrosidase mutations in Parkinson's disease. *N. Engl. J. Med.* **2009**, *361*, 1651–1661.

(3) Schapira, A. H. V.; Olanow, C. W.; Greenamyre, J. T.; Bezdud, E. Slowing of neurodegeneration in Parkinson's disease and Huntington's disease: future therapeutic perspectives. *Lancet* **2014**, *384*, 545–555.

(4) Sidransky, E.; Lopez, G. The link between the GBA gene and parkinsonism. *Lancet Neurol.* **2012**, *11*, 986–998.

(5) Lin, M. K.; Farrer, M. J. Genetics and genomics of Parkinson's disease. *Genome Med.* **2014**, *6*, 48.

(6) Sawkar, A. R.; Cheng, W.-C.; Beutler, E.; Wong, C.-H.; Balch, W. E.; Kelly, J. W. Nonlinear partial differential equations and applications: Chemical chaperones increase the cellular activity of N370S β -glucosidase: A therapeutic strategy for Gaucher disease. *Proc. Natl. Acad. Sci. U.S.A.* **2002**, *99*, 15428–15433.

(7) Grabowski, G. A. Phenotype, diagnosis, and treatment of Gaucher's disease. *Lancet* **2008**, *372*, 1263–1271.

(8) Bennett, L. L.; Mohan, D. Gaucher disease and its treatment options. *Ann. Pharmacother.* **2013**, *47*, 1182–1193.

(9) Mazzulli, J. R.; Xu, Y.-H.; Sun, Y.; Knight, A. L.; McLean, P. J.; Caldwell, G. A.; Sidransky, E.; Grabowski, G. A.; Krainc, D. Gaucher disease glucocerebrosidase and α -synuclein form a bidirectional pathogenic loop in synucleinopathies. *Cell* **2011**, *146*, 37–52.

(10) Sardi, S. P.; Clarke, J.; Viel, C.; Chan, M.; Tamsett, T. J.; Treleaven, C. M.; Bu, J.; Sweet, L.; Passini, M. A.; Dodge, J. C.; Yu, W. H.; Sidman, R. L.; Cheng, S. H.; Shihabuddin, L. S. Augmenting CNS glucocerebrosidase activity as a therapeutic strategy for parkinsonism and other Gaucher-related synucleinopathies. *Proc. Natl. Acad. Sci. U.S.A.* **2013**, *110*, 3537–3542.

(11) Sybertz, E.; Krainc, D. Development of targeted therapies for Parkinson's disease and related synucleinopathies. *J. Lipid Res.* **2014**, *55*, 1996–2003.

(12) Zheng, W.; Padia, J.; Urban, D. J.; Jadhav, A.; Goker-Alpan, O.; Simeonov, A.; Goldin, E.; Auld, D.; LaMarca, M. E.; Inglese, J.; Austin, C. P.; Sidransky, E. Three classes of glucocerebrosidase inhibitors identified by quantitative high-throughput screening are chaperone leads for Gaucher disease. *Proc. Natl. Acad. Sci. U.S.A.* **2007**, *104*, 13192–13197.

(13) Marugan, J. J.; Zheng, W.; Motabar, O.; Southall, N.; Goldin, E.; Westbroek, W.; Stubblefield, B. K.; Sidransky, E.; Aungst, R. A.; Lea, W. A.; Simeonov, A.; Leister, W.; Austin, C. P. Evaluation of quinazoline analogues as glucocerebrosidase inhibitors with chaperone activity. *J. Med. Chem.* **2011**, *54*, 1033–1058.

(14) Marugan, J. J.; Huang, W.; Motabar, O.; Zheng, W.; Xiao, J.; Patnaik, S.; Southall, N.; Westbroek, W.; Lea, W. A.; Simeonov, A.; Goldin, E.; DeBernardi, M. A.; Sidransky, E. Non-iminosugar glucocerebrosidase small molecule chaperones. *MedChemComm* **2012**, *3*, 56–60.

(15) Tropak, M. B.; Kornhaber, G. J.; Rigat, B. A.; Maegawa, G. H.; Buttner, J. D.; Blanchard, J. E.; Murphy, C.; Tuske, S. J.; Coales, S. J.; Hamuro, Y.; Brown, E. D.; Mahuran, D. J. Identification of pharmacological chaperones for Gaucher disease and characterization of their effects on β -glucocerebrosidase by hydrogen/deuterium exchange mass spectrometry. *ChemBioChem* **2008**, *9*, 2650–2662.

(16) Huang, W.; Zheng, W.; Urban, D. J.; Inglese, J.; Sidransky, E.; Austin, C. P.; Thomas, C. J. N4-phenyl modifications of N2-(2-hydroxyethyl)ethyl-6-(pyrrolidin-1-yl)-1,3,5-triazine-2,4-diamines enhance glucocerebrosidase inhibition by small molecules with potential as chemical chaperones for Gaucher disease. *Bioorg. Med. Chem. Lett.* **2007**, *17*, 5783–5789.

(17) Patnaik, S.; Zheng, W.; Choi, J. H.; Motabar, O.; Southall, N.; Westbroek, W.; Lea, W. A.; Velayati, A.; Goldin, E.; Sidransky, E.;

Leister, W.; Marugan, J. J. Discovery, structure-activity relationship, and biological evaluation of noninhibitory small molecule chaperones of glucocerebrosidase. *J. Med. Chem.* **2012**, *55*, 5734–5748.

(18) Mazzulli, J. R.; Zunke, F.; Tsunemi, T.; Toker, N. J.; Jeon, S.; Burbulla, L. F.; Patnaik, S.; Sidransky, E.; Marugan, J. J.; Sue, C. M.; Krainc, D. Activation of β -glucocerebrosidase reduces pathological α -synuclein and restores lysosomal function in Parkinson's patient midbrain neurons. *J. Neurosci.* **2016**, *36*, 7693–7706.

(19) Zheng, J.; Chen, L.; Schwake, M.; Silverman, R. B.; Krainc, D. Design and synthesis of potent quinazolines as selective β -glucocerebrosidase modulators. *J. Med. Chem.* **2016**, *59*, 8508–8520.

(20) Storz, T.; Heid, R.; Zeldis, J.; Hoagland, S. M.; Rapisardi, V.; Hollywood, S.; Morton, G. Convenient and practical one-pot synthesis of 4-chloropyrimidines via a novel chloroimidate annulation. *Org. Process Res. Dev.* **2011**, *15*, 918–924.

(21) Zheng, J.; Chen, L.; Skinner, O. S.; Ysselstein, D.; Remis, J.; Lansbury, P.; Skerlj, R.; Mrosek, M.; Heunisch, U.; Krapp, S.; Charrow, J.; Schwake, M.; Kelleher, N. L.; Silverman, R. B.; Krainc, D. β -Glucocerebrosidase modulators promote dimerization of β -glucocerebrosidase and reveal an allosteric binding site. *J. Am. Chem. Soc.* **2018**, *140*, 5914–5924.

(22) Zunke, F.; Andresen, L.; Wessler, S.; Groth, J.; Arnold, P.; Rothaug, M.; Mazzulli, J. R.; Krainc, D.; Blanz, J.; Saftig, P.; Schwake, M. Characterization of the complex formed by β -glucocerebrosidase and the lysosomal integral membrane protein type-2. *Proc. Natl. Acad. Sci. U.S.A.* **2016**, *113*, 3791–3796.

(23) Takahashi, K.; Tanabe, K.; Ohnuki, M.; Narita, M.; Ichisaka, T.; Tomoda, K.; Yamanaka, S. Induction of pluripotent stem cells from adult human fibroblasts by defined factors. *Cell* **2007**, *131*, 861–872.

(24) Seibler, P.; Graziotto, J.; Jeong, H.; Simunovic, F.; Klein, C.; Krainc, D. Mitochondrial Parkin recruitment is impaired in neurons derived from mutant PINK1 induced pluripotent stem cells. *J. Neurosci.* **2011**, *31*, 5970–5976.

(25) Kriks, S.; Shim, J.-W.; Piao, J.; Ganat, Y. M.; Wakeman, D. R.; Xie, Z.; Carrillo-Reid, L.; Auyeung, G.; Antonacci, C.; Buch, A.; Yang, L.; Beal, M. F.; Surmeier, D. J.; Kordower, J. H.; Tabar, V.; Studer, L. Dopamine neurons derived from human ES cells efficiently engraft in animal models of Parkinson's disease. *Nature* **2011**, *480*, 547–551.

(26) Burbulla, L. F.; Song, P.; Mazzulli, J. R.; Zampese, E.; Wong, Y. C.; Jeon, S.; Santos, D. P.; Blanz, J.; Obermaier, C. D.; Strojny, C.; Savas, J. N.; Kiskinis, E.; Zhuang, X.; Krüger, R.; Surmeier, D. J.; Krainc, D. Dopamine oxidation mediates mitochondrial and lysosomal dysfunction in Parkinson's disease. *Science* **2017**, *357*, 1255–1261.